

## 36 Appendix X – List of Priority Inspection Roads

**Table 90.** List of priority roads, by route ID (RTID) and status, for inspection to determine if they are actively eroding and delivering sediment to a stream.

RTID	STATUS	Length in Feet	RTID	STATUS	Length in Feet	RTID	STATUS	Length in Feet	RTID	STATUS
1S-8-1.0	BLOCKED	8,059	IDCK0.43	OPEN	1,169	BATE	OPEN	562	1-8-22.4	BLOCKED
JORDAN CK	OPEN	6,459	EAID	OPEN	1,167	1-8-1.24	BLOCKED	544	1-8-36.51	OPEN
ARCH CAPE MI	BLOCKED	5,685	1-7-11.1	BLOCKED	1,144	SF JORDAN	OPEN	536	2-8-26.1	OPEN
UFAL	OPEN	5,669	W FK WIL	OPEN	1,139	FOX	OPEN	532	LAMT2.12	OPEN
1-8-1.2	BLOCKED	5,424	1-7-11	OPEN	1,093	1S-8-4.1	BLOCKED	526	1S-7-11.2	OPEN
JUNO	OPEN	4,363	LAMT	OPEN	1,054	N FK WIL	OPEN	515	E ACCESS	OPEN
POLLO	BLOCKED	4,076	1-7-12.1	OPEN	1,026	UFAL4.13	OPEN	496	SFWI5.53	BLOCKED
OLD CDR	BLOCKED	3,274	1S-8-6.21	BLOCKED	1,009	1-7-36	BLOCKED	494	1-7-36	OPEN
SFWI1.42	OPEN	3,192	1-7-21.6	BLOCKED	980	1-7-36.3	BLOCKED	468	SFWI3.52D1	OPEN
RNHRT CK	BLOCKED	2,924	SMITH	OPEN	971	1S-8-6.3	BLOCKED	460	1-7-9.2	OPEN
KNS CK	OPEN	2,832	1-8-26.2	BLOCKED	966	SF JORDAN	BLOCKED	450	1S-8-4.1	OPEN
2-7-33.1	BLOCKED	2,731	2-8-26.2	OPEN	946	1S-8-4.16	BLOCKED	450	DRCK2.00	OPEN
D FNCE	BLOCKED	2,727	LIL NF	OPEN	923	2-7-15.31	BLOCKED	448	1S-8-8.5	OPEN
MING PT RD	OPEN	2,571	POWERLINE5	BLOCKED	913	SCCK0.53	BLOCKED	442	1-8-25.9	OPEN
1S-9-18.2	BLOCKED	2,527	2-8-24.0	BLOCKED	873	UFAL0.52	OPEN	439	1S-7-10.55	BLOCKED
LIL NF	BLOCKED	2,487	1S-8-5.0	BLOCKED	865	CLIN	OPEN	431	1-8-1.4	OPEN
YANKEE	BLOCKED	2,454	2-7-28	OPEN	862	1S-8-12.0	BLOCKED	430	1-8-36.5	OPEN
JONES	BLOCKED	2,437	HOSKINS	BLOCKED	859	2-8-25.2	BLOCKED	424	FALL CK	OPEN
GORGE RD	BLOCKED	2,330	1-7-33.4	OPEN	858	1S-7-10.5	OPEN	423	SFWI2.65A	OPEN
TILLISON CK	OPEN	2,285	1S-8-8.6	OPEN	836	CST RNG LP	OPEN	406	1-8-36.3	OPEN
BLU CK	BLOCKED	2,214	SFWI3.52D	OPEN	732	LAMT2.89	OPEN	400	1S-9-17.92	BLOCKED
CDR BTTE	OPEN	2,086	1-8-12.5	OPEN	730	1S-8-4.16	OPEN	400	1-8-21.4	BLOCKED
7CED2.25	OPEN	2,009	POWERLINE1	BLOCKED	727	KANSAS CK LP	OPEN	390	WOLF PT	OPEN
BEN SMITH	OPEN	1,976	1-8-1.21	BLOCKED	726	1-7-36.31	BLOCKED	386	RUTH1.39	BLOCKED
1-7-11.13	BLOCKED	1,899	WOLFCREEKRD	OPEN	718	1-8-12.5	BLOCKED	370	SAM DOWNS2	OPEN
1-8-23.1	BLOCKED	1,815	POWERLINE11	BLOCKED	710	IDCK1.56	OPEN	358	1-7-31.11	BLOCKED

RTID	STATUS	Length in Feet	RTID	STATUS	Length in Feet	RTID	STATUS	Length in Feet	RTID	STATUS
SAM DOWNS	BLOCKED	1,810	1-8-21.5	BLOCKED	707	DEDB0.22	OPEN	356	1-8-10.5	BLOCKED
2-8-24.1	OPEN	1,675	DEDB	OPEN	702	BLU RDG	OPEN	318	POWERLINE3	BLOCKED
BVR	OPEN	1,672	7CED	OPEN	693	SFWI1.42C	OPEN	311	1-8-19.7	OPEN
2-7-15.3	BLOCKED	1,626	1-8-2.8	BLOCKED	670	1-7-12.3	OPEN	311	2-7-7.3	BLOCKED
NF WF	OPEN	1,590	DRCK	OPEN	650	1-7-8.7	OPEN	304	2-7-17.12	OPEN
MILLS_BRDG	OPEN	1,515	1S-8-11.0	OPEN	640	ROGERS RD	BLOCKED	304	1-8-29.3	OPEN
1-8-25.1A	OPEN	1,498	SFWI2.65	OPEN	591	1-7-7.4	BLOCKED	303	POWERLINE10	BLOCKED
DMD	OPEN	1,399	1S-8-11.411	BLOCKED	591	UFAL6.21	BLOCKED	288	BLOW CK	OPEN
1-6-18.1	OPEN	1,306	1S-8-1.1	BLOCKED	586	BERRY	OPEN	285	1-7-9.2	BLOCKED
1-8-25.2	BLOCKED	1,301	D FNCE	OPEN	579	LYDA RD	OPEN	282	1-8-25.1A1	OPEN
CLIN5.51	BLOCKED	1,286	1-6-18	OPEN	570	LYDA RD1.11	OPEN	276	1-8-22.7	BLOCKED
1S-9-18.4	BLOCKED	1,216	KILCH LO	OPEN	563	KILCHIS LO	OPEN	273	1-8-33	BLOCKED
RUSH RD	BLOCKED	1,214								

## 37 Appendix Y – Potential Future Conditions: Riparian Modeling Scenarios and Comparisons

<b>37.1 POTENTIAL FUTURE CONDITIONS: RIPARIAN MODELING SCENARIOS .....</b>	<b>599</b>
37.1.1 Source Data.....	600
37.1.2 Canopy Live Tree Density Dynamics ( $\geq 14$ inches DBH) .....	601
37.1.2.1 Total Trees Per Acre (TPA) .....	601
37.1.2.2 Rate of Change in Total TPA.....	603
37.1.2.3 Conifer and Hardwood Canopy Structures.....	606
37.1.2.4 Conifer and Hardwood Understory Structures.....	611
37.1.3 Canopy Mortality Dynamics ( $\geq 14$ inches DBH).....	615
37.1.3.1 Total Canopy Mortality.....	615
37.1.3.2 Rate of Change in Canopy Mortality ( $\geq 14$ inches DBH) .....	618
37.1.3.3 Conifer and Hardwood Canopy Mortality.....	621
37.1.4 Compositional Dynamics.....	626
37.1.5 Key Findings.....	628
37.1.6 Conclusions Pertaining to the Watershed Analysis.....	629

### 37.1 Potential Future Conditions: Riparian Modeling Scenarios

Two growth projection model runs using the Forest Vegetation Simulator (FVS) were conducted to estimate the potential future conditions for the standing forest components for the Wilson River watershed. The first model involved the measured data collected from the growth-year field season of 2006 ( $\geq 5$  inches DBH), as presented as “Model #1” results in the Wilson River Watershed Analysis. The second model run involved these same data with a separate 0-5 inch DBH component and regeneration feature added to the projection (“Model #2”).

This addendum is organized in a similar fashion to the *Riparian Vegetation Dynamics: “No Management” Scenario* found in the Wilson Watershed Analysis, with data presented at the subwatershed (sixth-field) scale for Model #1 and Model #2. In addition, for most model output viewpoints, an evaluation of model differences was made. This is simply the difference in the outputs from both models; values below the X-axis ( $<0$ ) indicate responses where Model #2 was lower than Model #1. Conversely, values  $>0$  indicate where Model #2 responses were higher than #1. These values are mostly expressed on a trees per acre basis.

This addendum is presented to allow ODF to directly evaluate the changes in model outcomes from a range of riparian diagnostic viewpoints, presented at similar scales. Discussions follow as to how the two different model runs influence the conclusions of the riparian dynamics for the Wilson River system.

### 37.1.1 Source Data

Estimates of stand successional dynamics and the potential for large wood debris recruitment from riparian vegetation were generated from the riparian dataset with expanded stand metrics (ODF lands only). The data collected as part of this project contained stand-specific measures, expandable by the 10 most common vegetation classes (FPS codes) by land area that were found to occur in the watershed. These data contained tree species, size and density values for all species  $\geq 5$  inches DBH. These contained the source data for Model #1.

To supplement the understory components (0-5 inches DBH) of the system for Model #2, SLI plot location information were used to identify areas where plot data existed in the SLI database and in the mapped riparian zones. These plot-level data did not likely fall within the same sampled plot as the  $\geq 5$  inch DBH dataset described above, but plots were correspondent with the measured stand, when available. Plot level data were recompiled to the mapped riparian polygon stand numbers, and these data were appended to the existing measured stand data, where applicable. For non-measured stands (expanded stands), average values were used on the basis of like FPS codes, and applied to those stands with the appropriate overstory information.

A regeneration stand table was created for the purposes of providing the FVS model with the necessary inputs to produce seedlings as part of the model run. These data originated from a grand average of seedling SLI plot data found in riparian zones for the Wilson River watershed.

Following assembly of the measured and expanded input data by FPS code, the datasets were modeled for growth and tree mortality using the Pacific Coast variant of FVS. Species, size and density projections were modeled in 10-year increments, from 2006 (growth year of field measurement) to 2106. Regeneration was forced in the model using 20-year increments because an initial model run using default and stand density thresholds did not produce regenerating seedlings (i.e., thresholds were not met for the default settings).

Following this modeling, projected data from the model runs were expanded to the riparian polygons on ODF lands, on the basis of FPS codes for expansion stands, and by stand number for measured stands. As stated in the watershed assessment, these land areas constitute approximately 92% of the ODF riparian zone area. Data were summarized to the subwatershed scale and presented in 10-year increment windows to express changes through time (as opposed to 50- and 100- year summaries).

## 37.1.2 Canopy Live Tree Density Dynamics ( $\geq 14$ inches DBH)

### 37.1.2.1 Total Trees Per Acre (TPA)

Mid- and overstory canopy components were selected through the 100-year time series to illustrate the shifts in abundances for the dominant and co-dominant trees in the canopy strata. Tree sizes  $\geq 14$  inches DBH were considered to be “mid and overstory” components, as these size classes contain the majority of the basal area, or are most influential on basal area and stand-level structure within a given stand (shade, LWD components, etc). Absolute abundances (trees per acre, TPA) for all tree species were considered, and stand-level averages were weighted on the basis of acre contribution to each subwatershed.

**Model #1** (Figure 86): For the 100-year time series, the overall canopy tree abundances increase from a range of  $\sim 50 - 70$  trees per acre in 2006 to a maximum range of  $\sim 70 - 95$  in 2066. By the end of the time series, overall trees in the dominant and co-dominant canopy strata decrease to  $\sim 60 - 80$  trees per acre, representing only a slight increase in density from the current conditions. For the watershed as a whole, a ‘bi-modal’ distribution is present, where some subwatersheds express peak densities on either side of the 50-year mark.

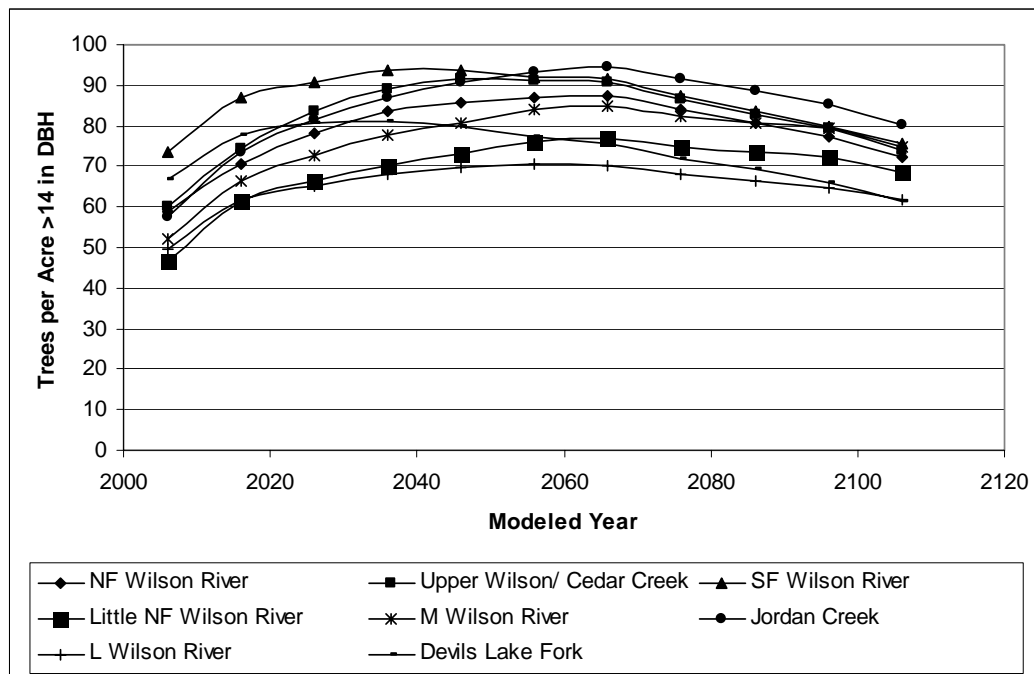


**Figure 86. Model #1** Projected Live Canopy Tree Densities. 100-year modeled weighted average standing trees per acre for conifers and hardwoods combined  $\geq 14$  inches DBH, reported by subwatershed.

**Model #2 (Figure 87):** Similar to Model #1, the trees per acre increase for the first 50-year period, and decrease for the second half of the 100-year model run. Overall canopy abundances follow similar total ranges (~50 – 95 TPA) to that of Model #1, with a decline occurring approximately 10 years earlier (2056 compared with 2066). The net TPA at the end of the model run is similar to that of Model #1, where total TPA decline to similar values to the beginning of the run, with slightly lower magnitude (60 – 80 vs. 50 – 65 TPA).

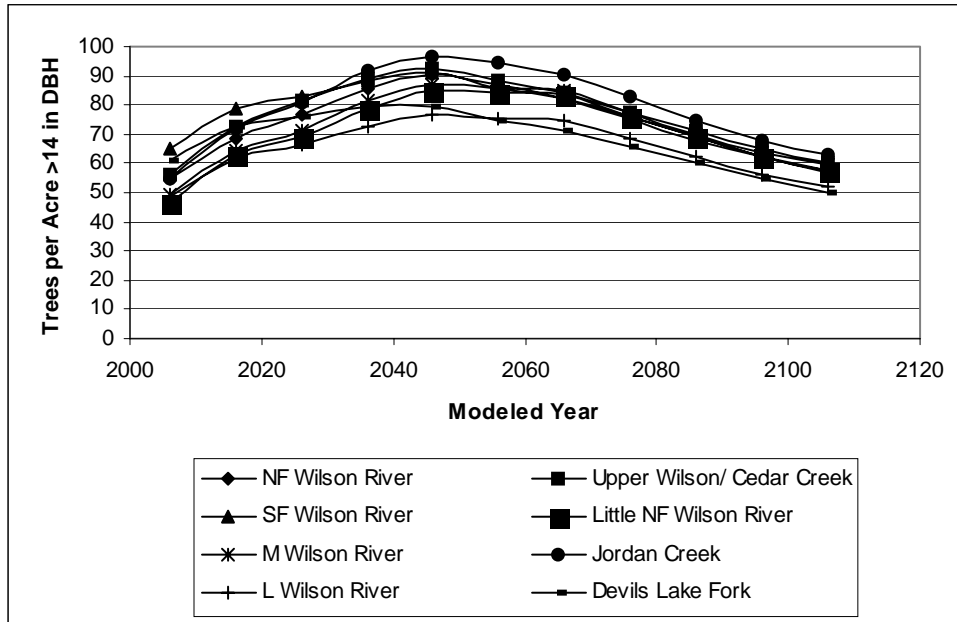


**Figure 87. Model #2.** Projected Live Canopy Tree Densities. 100-year modeled weighted average standing trees per acre for conifers and hardwoods combined  $\geq 14$  inches DBH, reported by subwatershed.

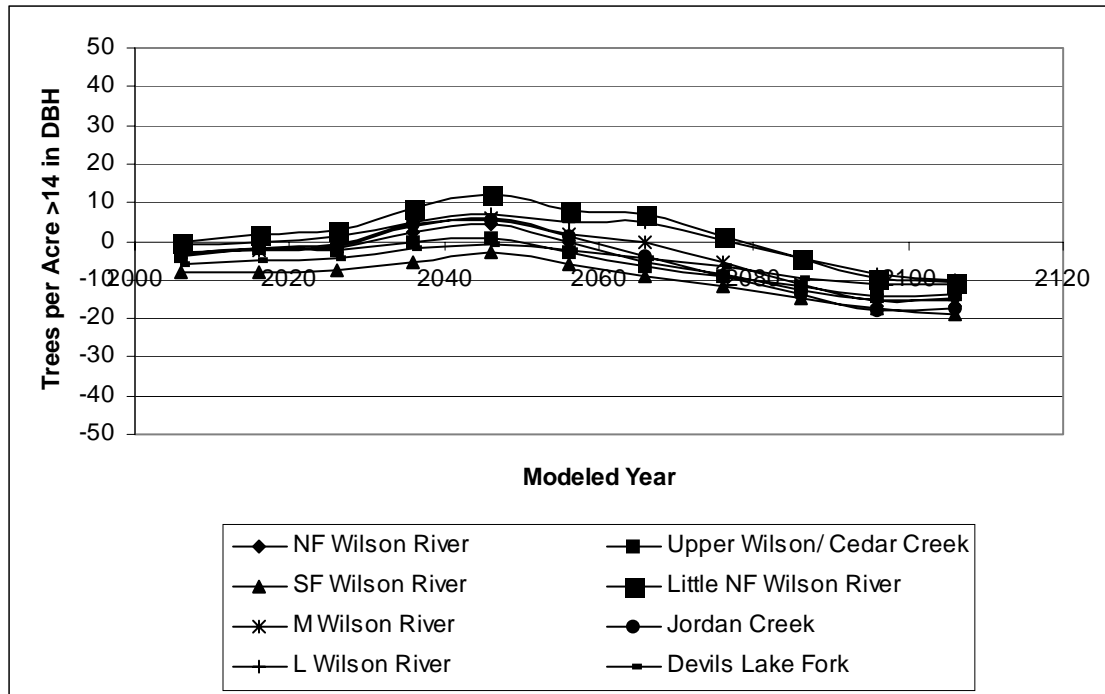


**Figure 88. Model Difference.** Projected Live Canopy Tree Densities. 100-year modeled weighted average standing trees per acre for conifers and hardwoods combined  $\geq 14$  inches DBH, reported by subwatershed.

**Model Differences (Figure 88):** TPA differences appear to be mostly relegated to the loss of a “bi-modal” distribution in TPA between 2036 and 2066 found in the Model 1 output to a single peak between 2036 and 2056. Also of note, Model #2 exhibits approximately 10 TPA less than Model #1 as the model run exceeds 80 years, and declines to a range of 10-20 fewer TPA in the last 20-year time steps as compared with Model #1 (evidenced by negative values in Figure 88). This is most likely due to the increase in total stand density values (because of the additional younger cohorts), contributing to model thresholds of stand density/ mortality triggers.

### 37.1.2.2 Rate of Change in Total TPA

Another useful measure of structural dynamics and the evaluation of model sensitivities involves calculating the rate of change in recruitment to a particular size class, expressed as a percentage. Rates of “canopy recruitment”, or the percentage increase (or loss) of trees entering the  $\geq 14$  inch DBH size class in a 10-year period were calculated for both model runs. This is the analogous to the percent slope (and slope direction) for the curves presented in Figure 89 and Figure 90 with a comparison presented in Figure 91.

**Model #1 (Figure 89):** The levels for canopy recruitment show rapid rates of recruitment in the first ~25 years, following a steady rate of decline by the end of

Year 50. Following modeled year 2066, the rates of change in canopy recruitment become sporadic and negative, indicating growth stagnation and lack of recruitment of younger trees into the canopy size class.

**Model #2 (Figure 90):** Similar to Model #1, there is an overall decline in the rate of recruitment to the canopy, though there is an increased recruitment by 2036, followed by a gradual decline to the end of the first 50 year period. In the 50-100 year time steps, canopy tree recruitment rates decline steadily and level off at a steady decline of 10% per model step for the final 30 years of the projection.

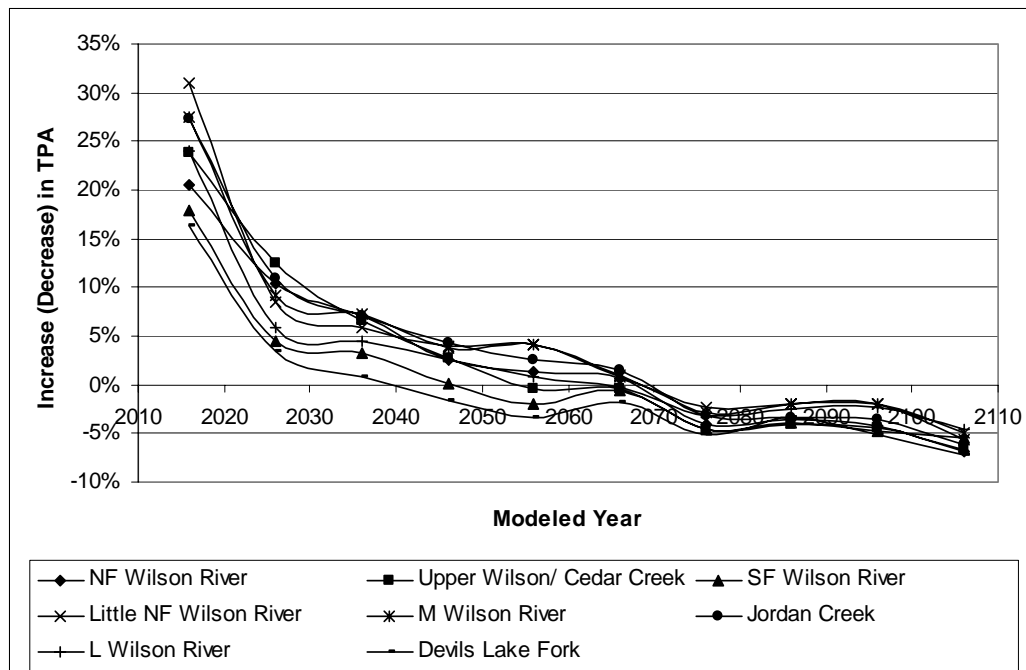


**Figure 89. Model #1:** Projected Rates of Live Canopy Tree Recruitment. The percent increase or decrease in TPA for trees  $\geq 14$  inches DBH through time. Note negative values show declines in recruitment rates to this size class.

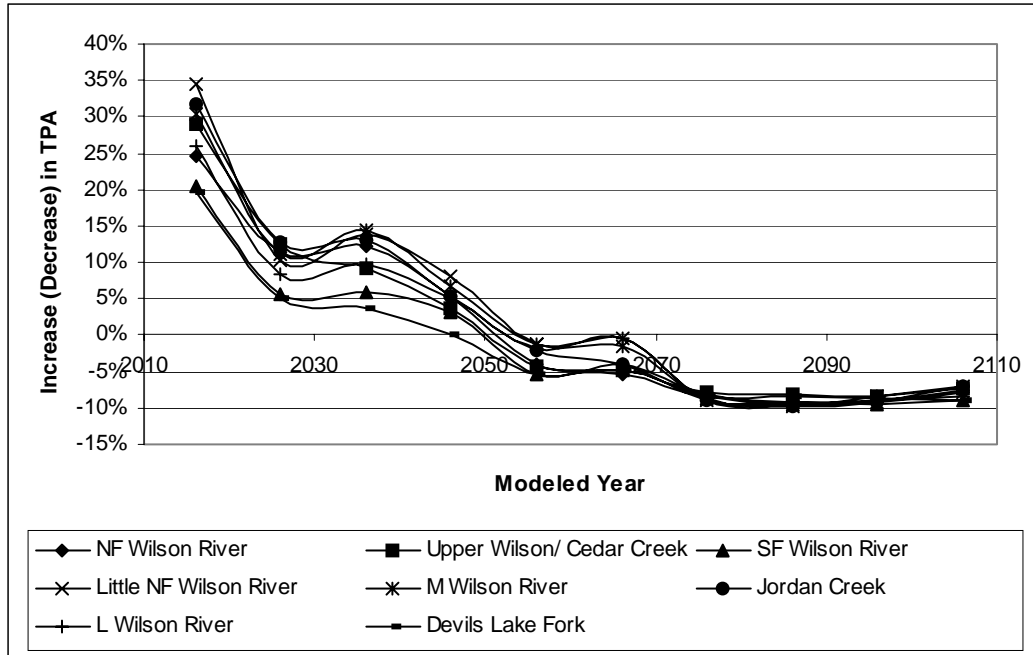


**Figure 90. Model #2:** Projected Rates of Live Canopy Tree Recruitment. The percent increase or decrease in TPA for trees ≥14 inches DBH through time. Note negative values show declines in recruitment rates to this size class.

**Model Differences (Figure 91):** The differences in recruitment rates to the canopy show a relative “flip” in temporal position for two models. Model #2 shows a 3 – 12% increase in canopy recruitment over Model #1 in the 20-40 year time steps; this is reversed with a ~5% difference when Model #1 declines in TPA at a slower rate than Model #2, beginning after year 50 (negative numbers) until the end of the model run. The total magnitude of these differences is approximately 5-7% for the latter half of the run.

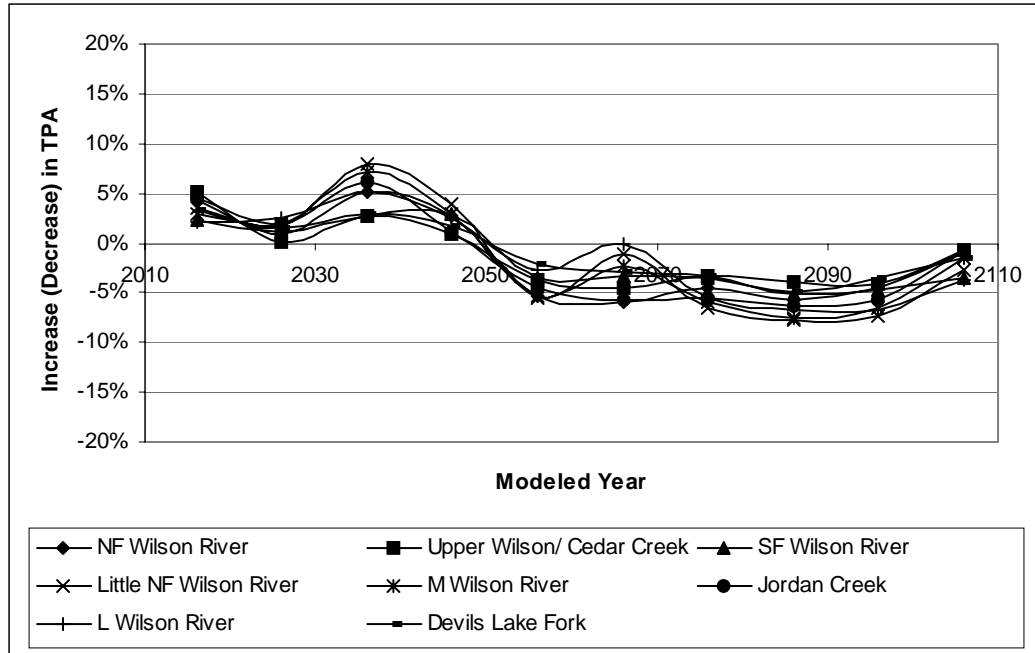


**Figure 91. Model Difference:** Projected Rates of Live Canopy Tree Recruitment. The percent increase or decrease in TPA for trees  $\geq 14$  inches DBH through time. Note negative values show declines in recruitment rates to this size class.

### 37.1.2.3 Conifer and Hardwood Canopy Structures

Similar to the analysis above, stem density information was further separated into conifer and hardwood species to examine the response of these species groups to the canopy size classes ( $\geq 14$  inches DBH).

**Model #1. Conifers (Figure 92).** The projected densities for live conifer recruitment to the canopy ( $\geq 14$  inches DBH) illustrate a slight increase in conifer recruitment within the first 10 years, followed by a steady decline over the remainder of the time period. In the time steps 2040 – 2060 (on either side of the 50 year mark), the conifer density in the canopy declines to approximately that found in the current conditions for all subwatersheds, resulting in a net loss of canopy-sized conifers by the end of the time period. Both SF Wilson and Devils Lake Fork, the richest in conifer abundances, are projected to have the largest nominal decline, ending the model run at a density lower than the highs of the conifer poor areas.

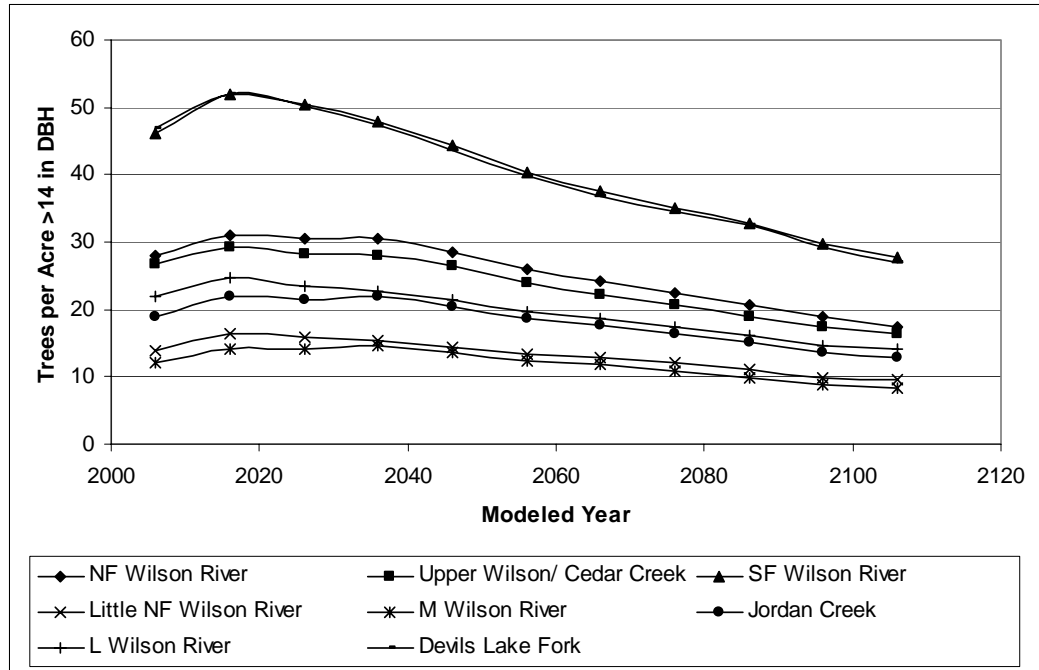


**Figure 92. Model #1:** Projected Conifer Recruitment to the Canopy (>14 inches DBH). 100-year modeled weighted average live conifer trees per acre for riparian zones on ODF lands.

**Model #2. Conifers (Figure 93).** Conifer densities follow similar patterns to Model #1, showing near-term peaks and gradual declines to pre-model levels. Ranges of TPA at their peaks for all subwatersheds are similar, though the magnitude of TPA in conifers for the SF Wilson and Devils Lake Fork subwatersheds dropped slightly, from the output associated with Model #1 (more discussion on this below).

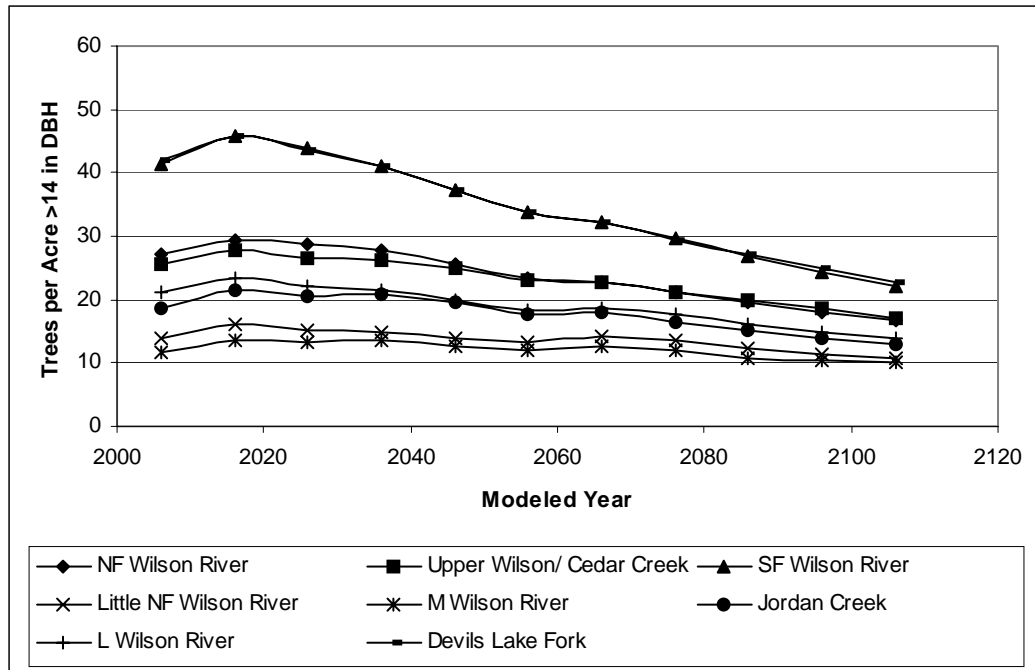


**Figure 93. Model #2:** Projected Conifer Recruitment to the Canopy (>14 inches DBH). 100-year modeled weighted average live conifer trees per acre for riparian zones on ODF lands.

**Model Differences. Conifers (Figure 94).** As expected from Figure 92 and Figure 93, the model differences did not show appreciable divergence in the two runs. Both the magnitude and the trends of the projected data are within similar tolerances. The SF Wilson and Devils Lake Fork (the most conifer rich) show an immediate but consistent bias in magnitude throughout the model run. Because of the consistency in the bias, this is likely a legacy of classifications in the database, where the precision of the compiled data may have placed a few tree records in the younger size class (e.g. the precision of 13.96 in one database caused promotion to the  $\geq 14$  inch class and to the  $< 14$  inch class in the other model run)<sup>1</sup>, or an early mortality event was triggered due to stand density thresholds. The net result shows a very consistent pattern in conifer canopy densities through time.

<sup>1</sup> Further examination is required to determine the cause of this bias.

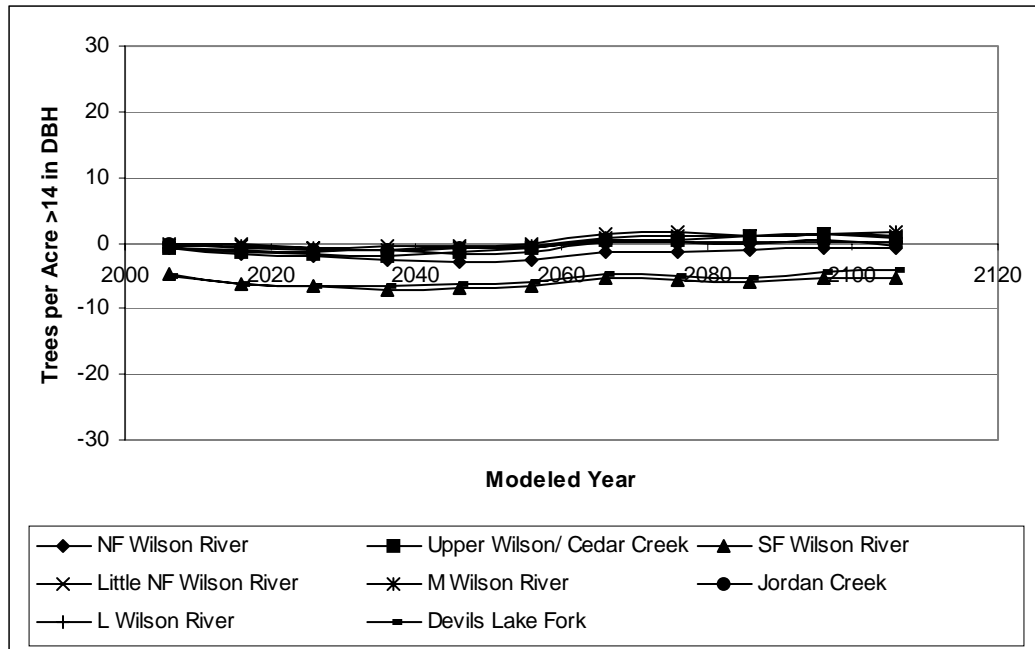


**Figure 94. Model Differences:** Projected Conifer Recruitment to the Canopy (>14 inches DBH). 100-year modeled weighted average live conifer trees per acre for riparian zones on ODF lands.

**Model #1. Hardwoods (Figure 95).** Live hardwood projections (TPA  $\geq 14$  inches DBH) show a near doubling in TPA by 2066, following with a gradual decline to the end of the model run. These curves appear to be the moderating component to the total TPA curves (Figure 1 series), showing approximately 2-1 ratios of hardwoods to conifers in these size classes. This is consistent with the amount of acres in hardwood co-dominance found within the Wilson watershed for the majority of the land area. At the end of the run, the hardwood component increases ~15 TPA between 0 and 100 years.

**Model #2. Hardwoods (Figure 96).** Likewise with Model #1, the TPA curves for hardwoods closely resemble the projected trends for total canopy TPA. Model #2 shows a consistent and steady rise and fall in hardwood density throughout the projection, with the peak hardwood densities occurring at approximately the 50-year time step. The magnitude in hardwood canopy densities is similar to Model #1 (20 – 80 TPA), with the key difference being in the timing and distribution of the peak (10 years earlier). Additionally, hardwoods comprise less of a component to the canopy (in absolute terms) at the end of the projection, as compared with Model #1. Overall, there is a small net increase in hardwood densities between year 0 and 100 (~10 TPA).

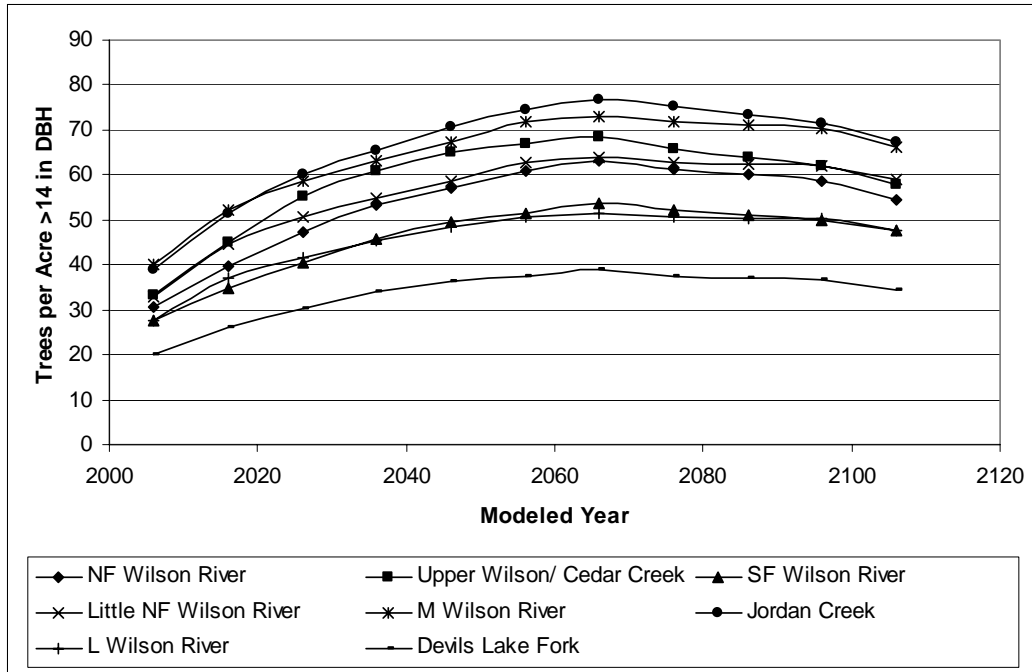


**Figure 95. Model #1:** Projected Hardwood Recruitment to the Canopy (>14 inches DBH). 100-year modeled weighted average live hardwood trees per acre for riparian zones on ODF lands.

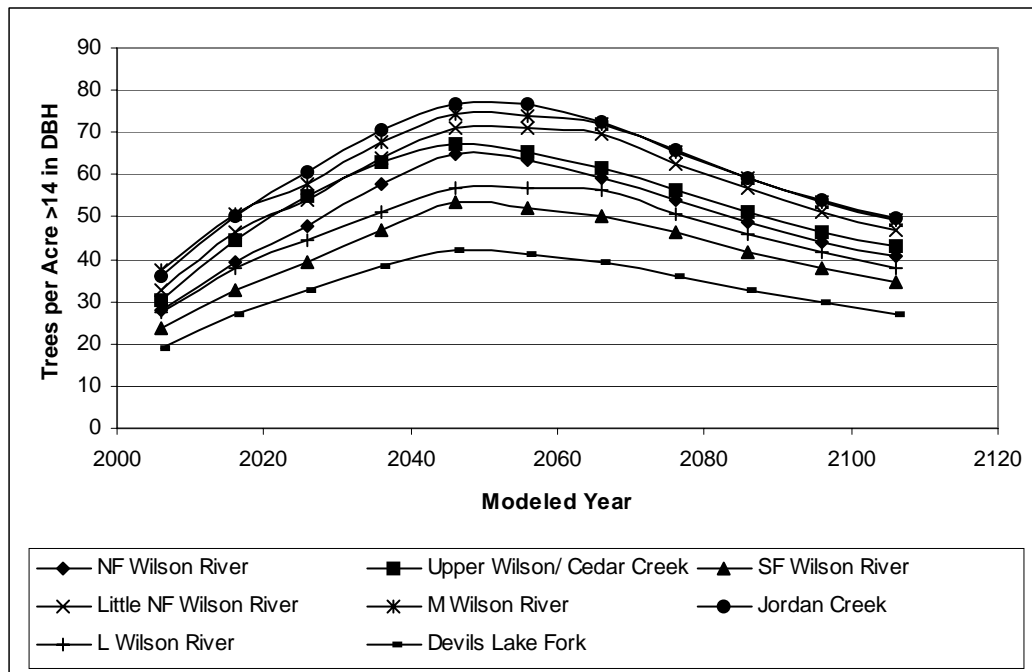


**Figure 96. Model #2:** Projected Hardwood Recruitment to the Canopy (>14 inches DBH). 100-year modeled weighted average live hardwood trees per acre for riparian zones on ODF lands.

**Model Differences. Hardwoods (Figure 97).** The magnitude shifts in timing of the hardwood peaks are most notable in ~2046 and again in ~2066 (though less consolidated (on either side of the 50-year time step). This difference in modeled TPA suggests the slightly ‘bimodal’ distribution of Model #1 and the single-peak event in Model #2 are related to hardwood densities and potentially competitive factors from younger cohorts (see subsequent sections). Though temporal changes exist (~10 years), the changes in magnitude for hardwood abundances in the canopy are within reasonable levels of one another.

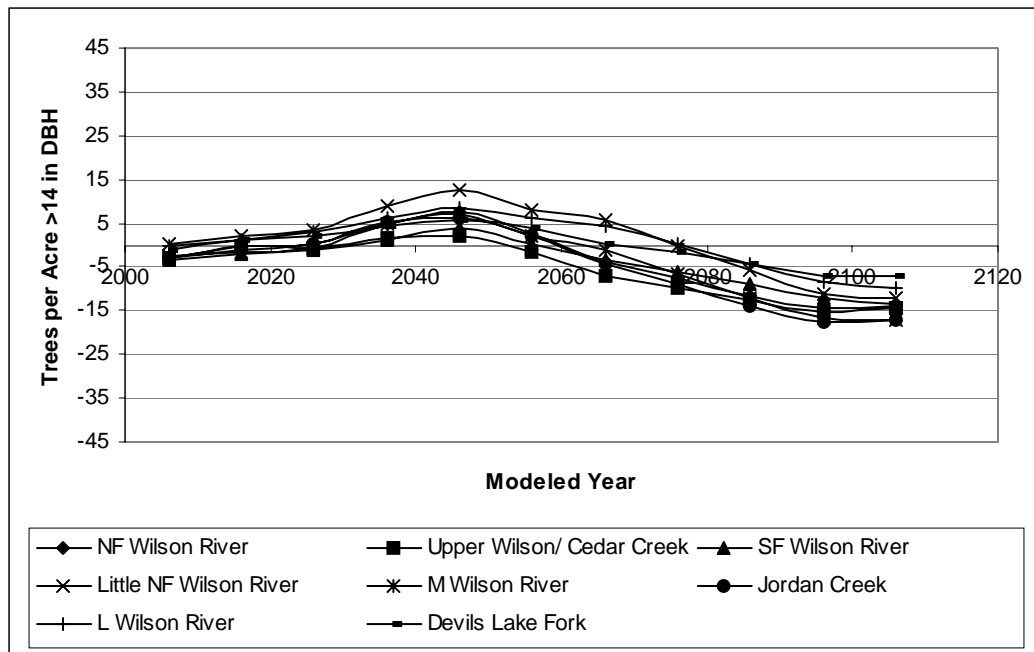


**Figure 97. Model Differences:** Projected Hardwood Recruitment to the Canopy (>14 inches DBH). 100-year modeled weighted average live hardwood trees per acre for riparian zones on ODF lands.

#### 37.1.2.4 Conifer and Hardwood Understory Structures

Similar to the canopy structural dynamics described in the previous section, understory structures and recruitment (defined as trees <14 inches DBH) were evaluated as subsets of conifers and hardwoods. Because the differences in the model runs centered on the absence (Model #1) and presence (Model #2) of small-diameter trees (0-5 inches DBH), the model runs are graphically compared as separate runs only, and not displayed with absolute differences in magnitude. Though graphed as separate species components for each model, the discussion incorporates both conifers and hardwoods in the model run assessment.

**Model #1. Conifers and Hardwoods <14 inches DBH (Figure 98 and Figure 100).** These size classes for conifers and hardwoods illustrates high values in the first ~30 years, contributing to the peaks of canopy recruitment and overall abundances before 2066. Notably, young hardwood densities are approximately 3 times higher in the early years of the cycle, and, though these values decrease, young hardwood densities are over five-fold the conifer density in the same size class by the end of the model period. These values represent tree size classes between 5 and 14 inches, or the lower canopy structure.

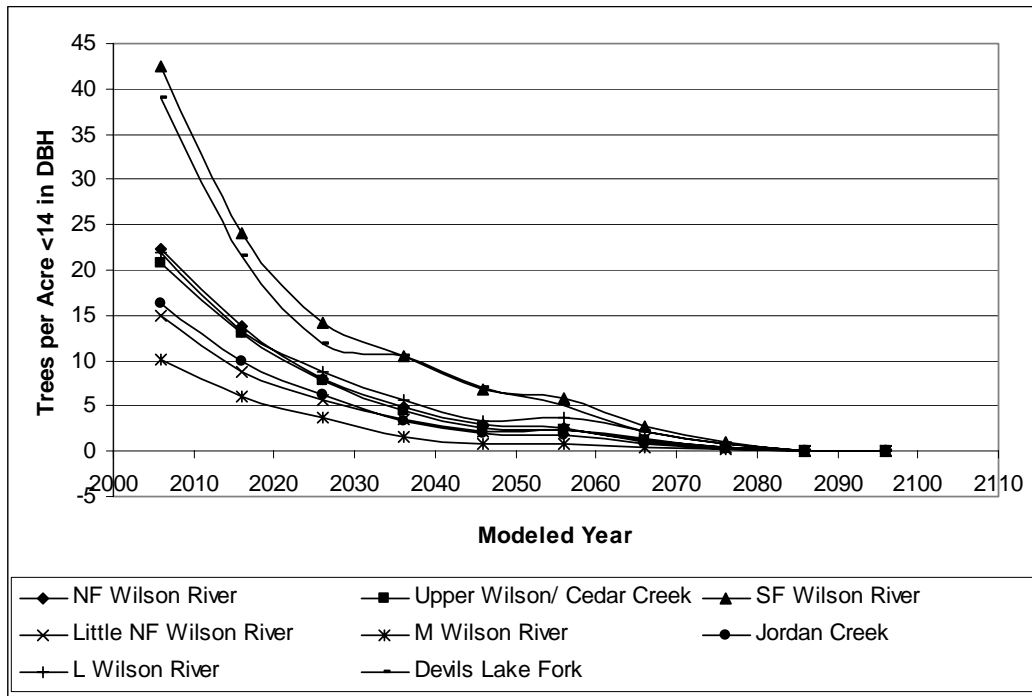


**Figure 98. Model #1.** Projected Conifer Understory. The 100-year projected density of conifer trees per acre in size classes <14 inches DBH. Mean values are weighted for acreage contribution by subwatershed.

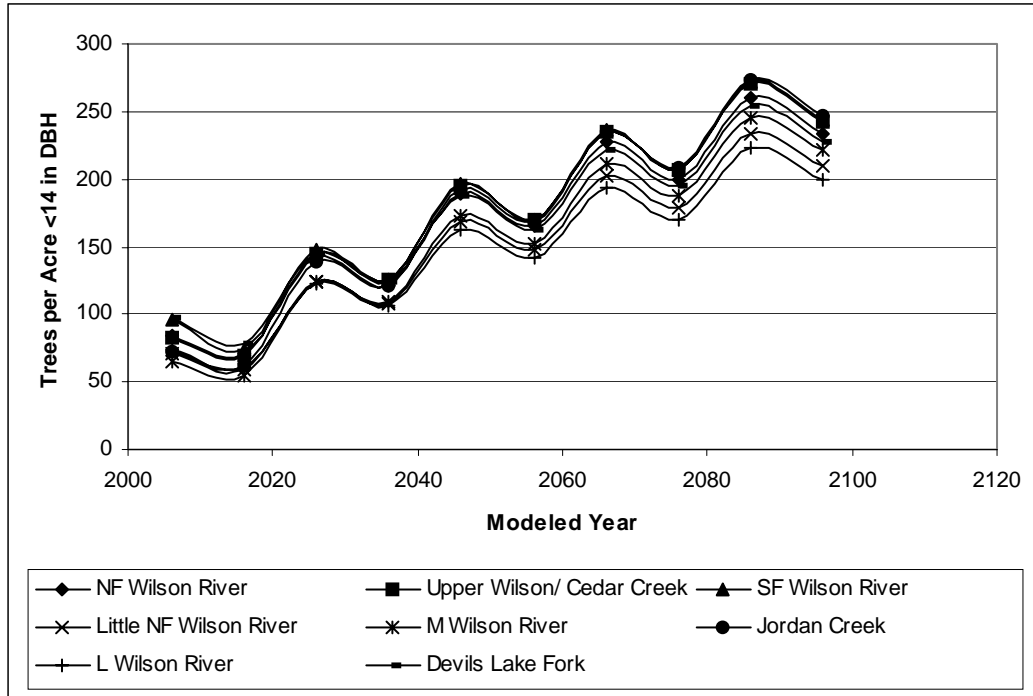


**Figure 99. Model #2.** Projected Conifer Understory. The 100-year projected density of conifer trees per acre in size classes <14 inches DBH. Mean values are weighted for acreage contribution by subwatershed.

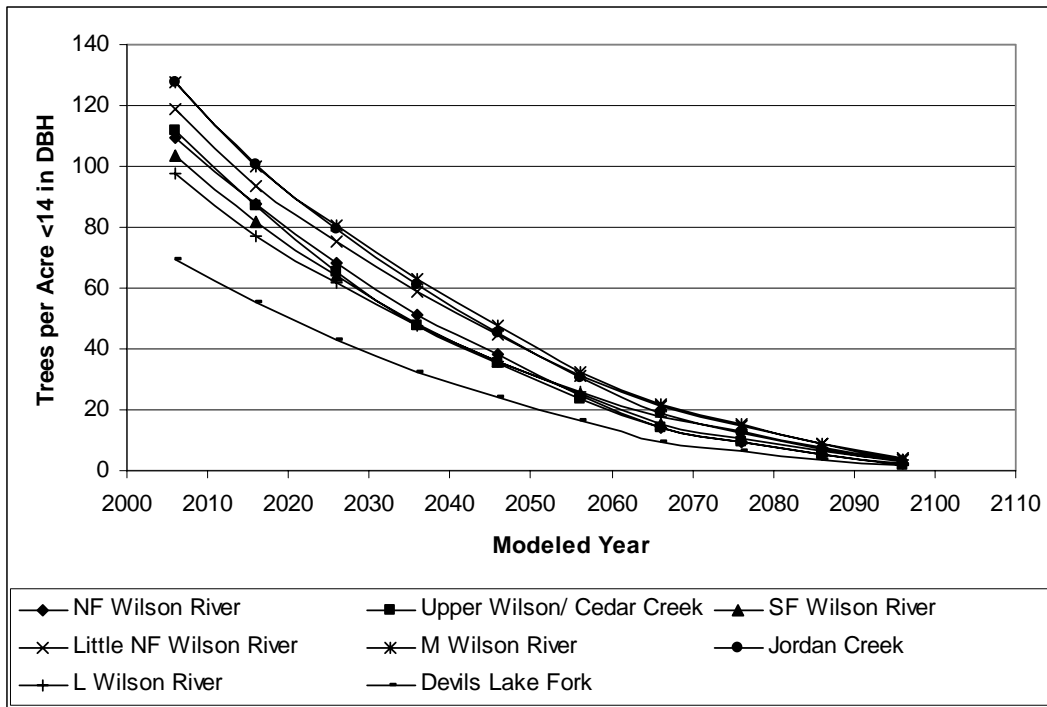


**Figure 100. Model #1.** Projected Hardwood Understory. The 100-year projected density of hardwood trees per acre in size classes <14 inches DBH. Mean values are weighted for acreage contribution by subwatershed.

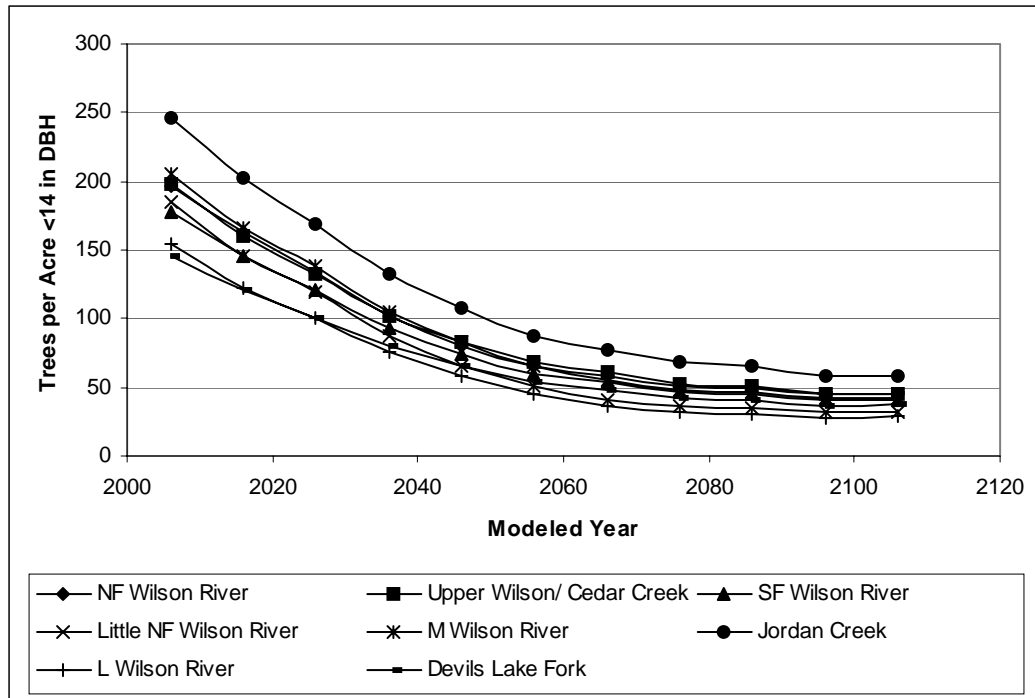


**Figure 101. Model #2.** Projected Hardwood Understory. The 100-year projected density of hardwood trees per acre in size classes <14 inches DBH. Mean values are weighted for acreage contribution by subwatershed.

**Model #2. Conifers and Hardwoods <14 inches DBH (Figure 99 and Figure 101).** Inclusion of the <5 inch size classes and the forced seedling establishment at regular intervals is best observed in the conifer regeneration graph (Figure 99), where steady increases in this size class proceed through the model run. Seedling regeneration is noticed by every-other time series runs (stair-step spike), with a corresponding drop in TPA (stair-step drop). This pattern is attributed to the projection model reaching stand density thresholds to promote self-thinning. In addition, the regeneration and 0-5 inch dataset was gathered from a different data source than the field measures (the SLI database). Though differences existed across the vegetation code spectrum for the <5 size class, the uniformity in magnitudes in the conifer curves in the early phases of the model run do not indicate much divergence among subwatersheds until the second half of the projection (>50 years). The subtle change among subwatersheds appears to be due to persistent species (e.g. hemlock) and areas where canopy densities are the highest (see year 50, Figure 87). The magnitude of the conifer curve in combination with the canopy recruitment models presented earlier suggests that this size class distribution probably (1) contains sufficient stocking to not be limited for potential canopy recruitment but is (2) probably limited in stand density indices driving growth and mortality thresholds. This suggests the model will inherently favor the most shade-tolerant conifer species. The hardwood

understory component (Figure 101) follows a similar decline as Model #1, with a magnitude approximately twice that of Model #1. Overall, the model run involving these <5 inch size classes contributes a “front end load” of conifers that increases through time; their recruitment to the canopy is most likely limited by the stand density thresholds to accommodate recruitment to larger size classes.

**Model Differences. Conifers and Hardwoods <14 inches DBH (no graphs presented).** The clear differences and consequences of additional data in the 0-5 inch DBH size classes, coupled with a forced regeneration component<sup>2</sup>, will always produce different projections than a dataset without these components. The clearest differences are in the magnitude of understory components (2x in hardwoods and >10x in conifers), and the stocking increases in understory conifers through the time series. Overall, the data suggest the model run maximizes conifer stocking and availability to recruit to larger size classes, though evidenced by the similarity in outputs for Models #1 and 2 in the ≥14 inch size classes, self-thinning, species persistence, and growth stagnation are probably being limited by model-driven stand density index thresholds.

### 37.1.3 Canopy Mortality Dynamics (≥14 inches DBH)

#### 37.1.3.1 Total Canopy Mortality

Mortality rates, expressed as trees per acre, were calculated for the 100-year time period for both model runs. The mortality rates expressed are through modeled mortality due to stem exclusion, competitive pressures, and other successional probabilities for mortality – mostly driven by stand density thresholds set in the FVS model<sup>3</sup>. A fundamental assumption is these estimates do not include stochastic events such as landslides, debris torrents, flooding, insects or disease, or fire. In addition, human-caused damages are not a factor, including harvest, compaction, recreational impacts, road damage, etc. Hence, these mortality estimates (and the standing live estimates for that matter) are framed in the fundamental assumption that disturbances will not occur for the 100-year time period.

The purpose of modeling mortality is to address what potential wood debris may contribute to the stream system, excluding active management and disturbance scenarios. Canopy tree species (≥14 inch size class) were targeted for this analysis because they are the most likely to contribute to the ecosystem services

---

<sup>2</sup> An additional model run (not presented here) was conducted with natural seedling establishment based on a normalized stand density threshold (e.g. under 80% of normal will initiate regeneration). This model run did not produce regeneration seedlings for the length of the model run; consequently “forced regeneration” and regular time step intervals was used to ensure the seedling component was considered in this analysis.

<sup>3</sup> Default values were used for both model runs.

of the stream system; the data presented in this section describes the potential mortality, of which a subset is potentially interactive with the stream channel. As in prior sections of this addendum, mortality is expressed as TPA, for both conifer and hardwood species, and scaled as a weighted average at the subwatershed level.

**Model #1. Canopy Mortality (All trees ≥14 inches DBH) (Figure 102).** As with standing live trees per acre, the projected mortality rates follow the pattern of moderate increases in mortality in the first ~30 years, followed by a general decline in dead trees per acre as the projection continues to the 100 year period. On average, the dead: live tree ratio for this size class under the Model #1 scenario is 10.6% (range 7.8 – 13.2%) among subwatersheds among all years. At the end of the model run, canopy mortality decreases in TPA to levels at or below the beginning of the projection.

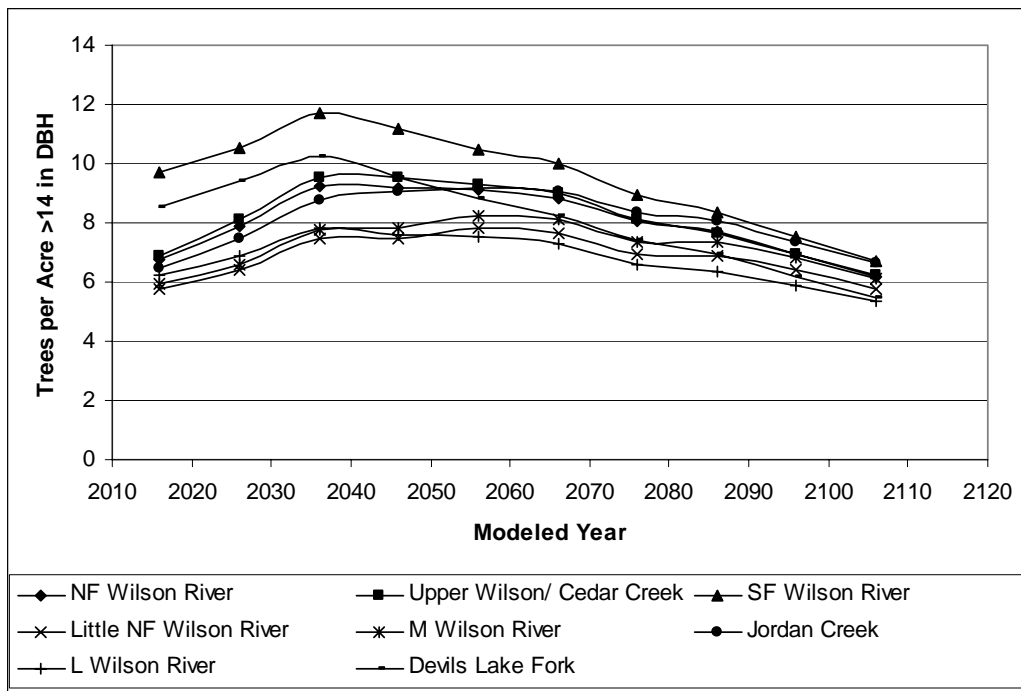


**Figure 102. Model #1** Projected Canopy Strata Mortality. 100-year modeled weighted average of dead trees ≥14 inches DBH per acre for conifers and hardwoods combined, presented by subwatershed.

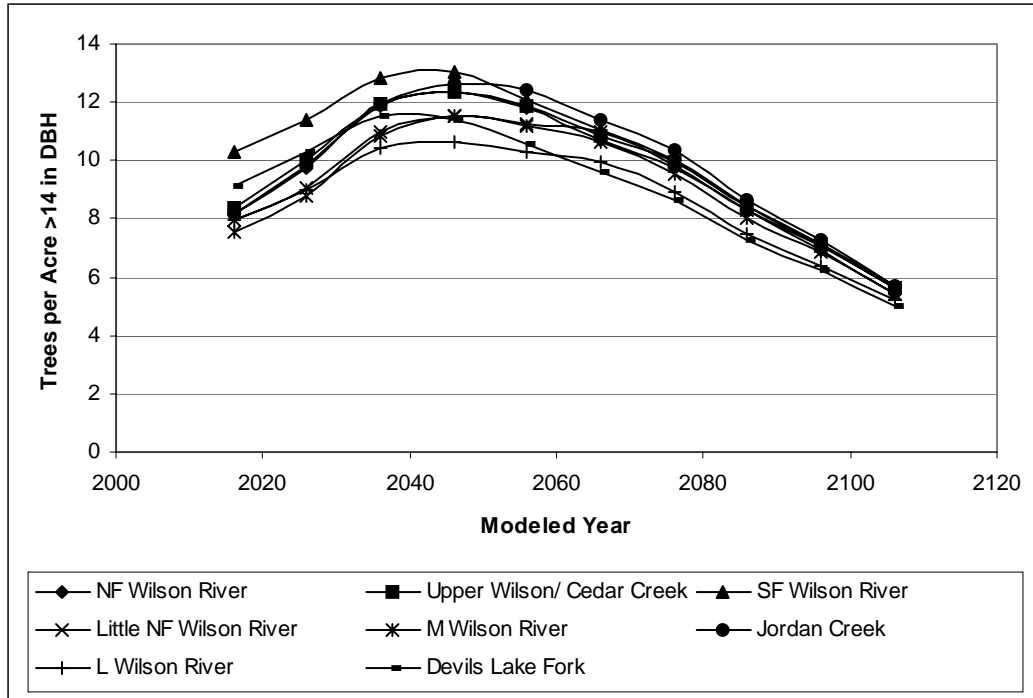


**Figure 103. Model #2.** Projected Canopy Strata Mortality. 100-year modeled weighted average of dead trees  $\geq 14$  inches DBH per acre for conifers and hardwoods combined, presented by subwatershed.

**Model #2. Canopy Mortality (All trees  $\geq 14$  inches DBH) (Figure 103).** In the same manner as Model #1, the second model run mirrored the trends associated with the live trees, showing moderate increases in dying trees, achieving a peak at  $\sim 40$  years, and declining steadily to the end of the projection. At the end of the projection, the dead TPA in this size class declined to approximately two-thirds of the levels from the beginning of the model run. The dead: live tree ratios for all years and subwatersheds averaged 12.7% (range 8.4 – 16.9%).

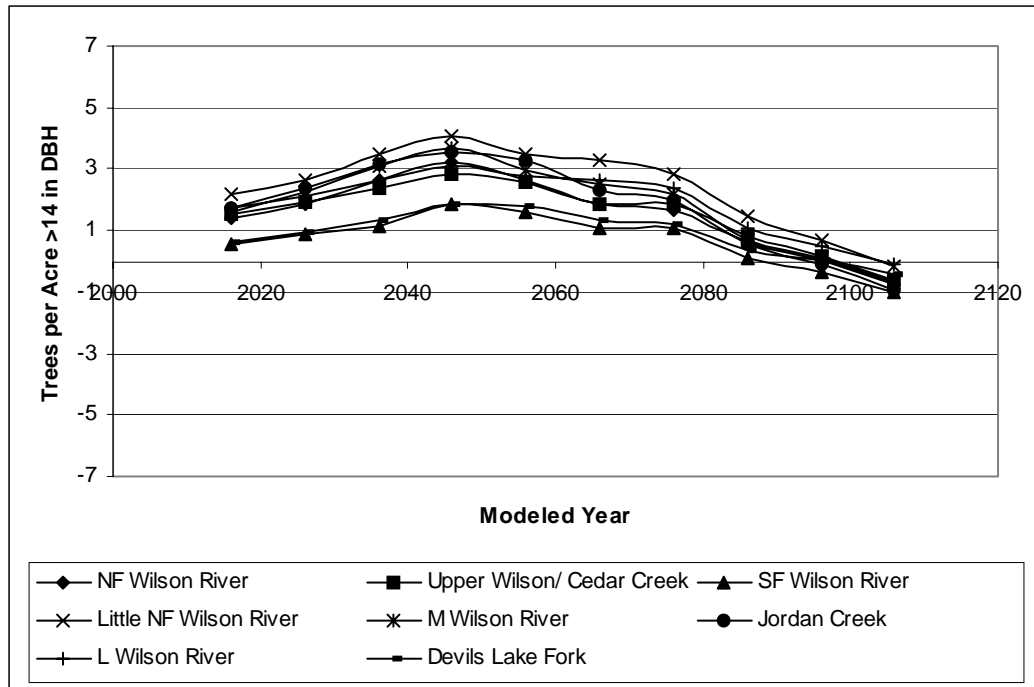


**Figure 104. Model Differences:** Projected Canopy Strata Mortality. 100-year modeled weighted average of dead trees  $\geq 14$  inches DBH per acre for conifers and hardwoods combined, presented by subwatershed.

**Model Differences. Canopy Mortality (All trees  $\geq 14$  inches DBH) (Figure 104).** Both model runs followed the similar trends of the live TPA component for the canopy size class. The primary difference was a steady and even increase in mortality for Model #2 versus Model #1. Toward the end of the projection, the model responses became more in-line (i.e. zero magnitude difference). The primary reasons for this observed change between Models #2 and #1 is the increase in mortality rates, generated from thresholds associated with stand density and mortality triggers in the FVS model. While the mortality is indeed higher under the Model #2 scenario for the majority of the time series, this bias remains somewhat consistent in magnitude (1-3 TPA).

### 37.1.3.2 Rate of Change in Canopy Mortality ( $\geq 14$ inches DBH)

In a similar fashion to live TPA, rates of change in canopy mortality were calculated for the model run to evaluate differences in slope and slope direction of the mortality curves.

**Model #1. Canopy Mortality Rate of Change (Figure 105).** Increases in mortality are dramatically reduced from Year 0 to 50 under this model scenario, with short pulses in mortality at the 50 year and 80 year marks. These are likely

events when the cohort establishment from the 5-14 inch DBH classes (as measured in 2006) begins to enter the upper canopy. Despite these pulses, the negative trending in mortality is dominant beginning years 30 – 50 for most subwatersheds (negative numbers in Figure 105).

**Model #2. Canopy Mortality Rate of Change (Figure 106).** This model scenario shows a higher pulse in mortality in the first few decades of the model run, followed by a steady and uniform decrease in mortality rates through time. At approximately Year 50, the rate of change in mortality slows considerably, at a rate of 10 – 20% less mortality with each passing decade between years 50 and 100. This suggests the stand densities have equilibrated to a point where tree ages are such that competition between younger and older cohorts is minimized.

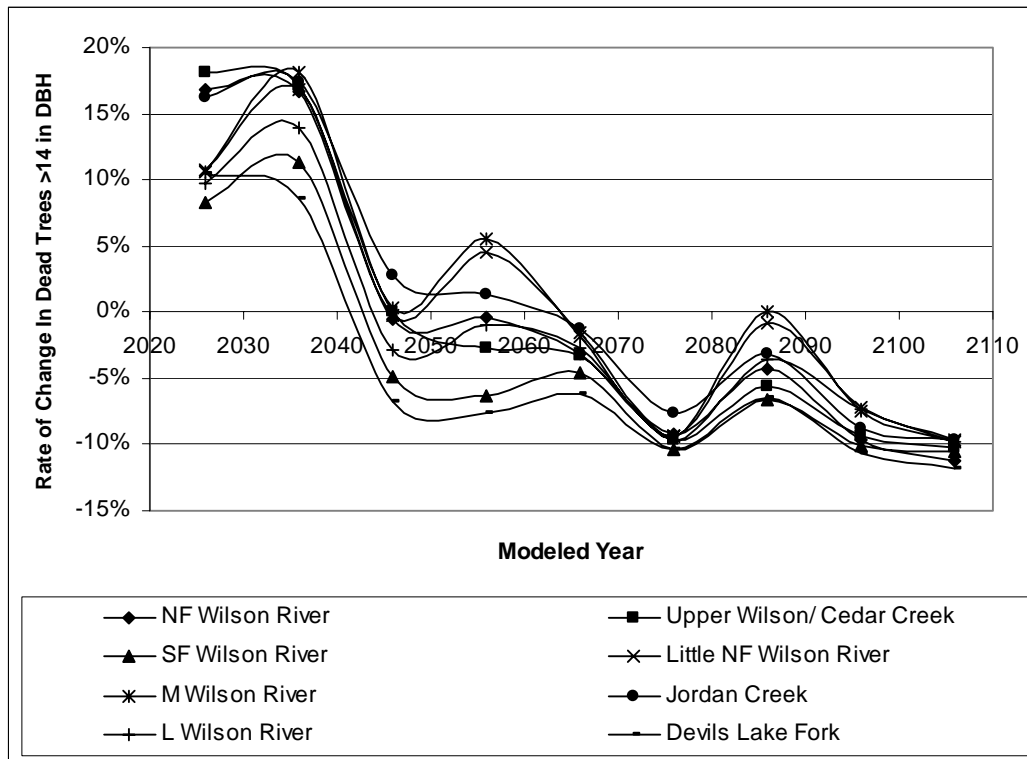


**Figure 105. Model #1.** Rate of Change in Canopy Tree Mortality. Percent increase or decrease in tree mortality  $\geq 14$  inches DBH, presented as weighted averages by subwatershed.

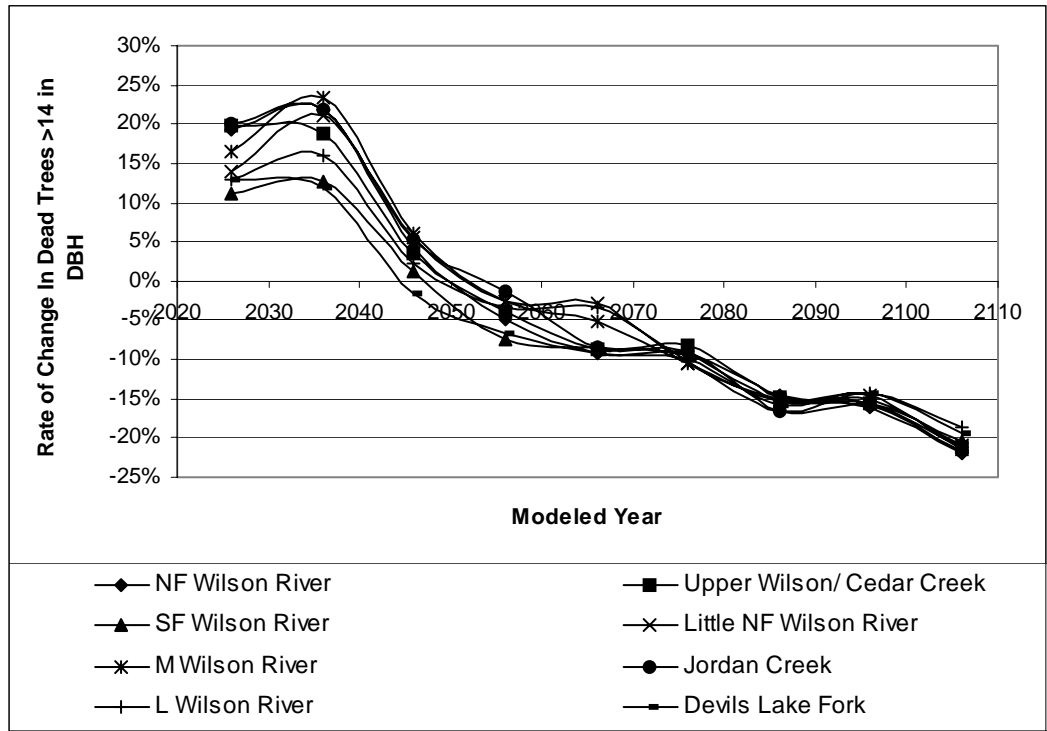


**Figure 106. Model #2.** Rate of Change in Canopy Tree Mortality. Percent increase or decrease in tree mortality  $\geq 14$  inches DBH, presented as weighted averages by subwatershed.

**Model Differences. Canopy Mortality Rate of Change (Figure 107).** Both models express a pulse in the beginning of the time series, followed by a steady decline in mortality rates through time. Model #1 shows a pulse of mortality events near years 50 and 80; these are evidenced by short diversions in Figure 8c. Overall, the magnitude of the mortality rate is within 10% between the two model runs; Model #2 has slightly higher TPA mortality densities, but the pattern of mortality (and suggested lag in available wood for LWD recruitment) is supported by both model runs.

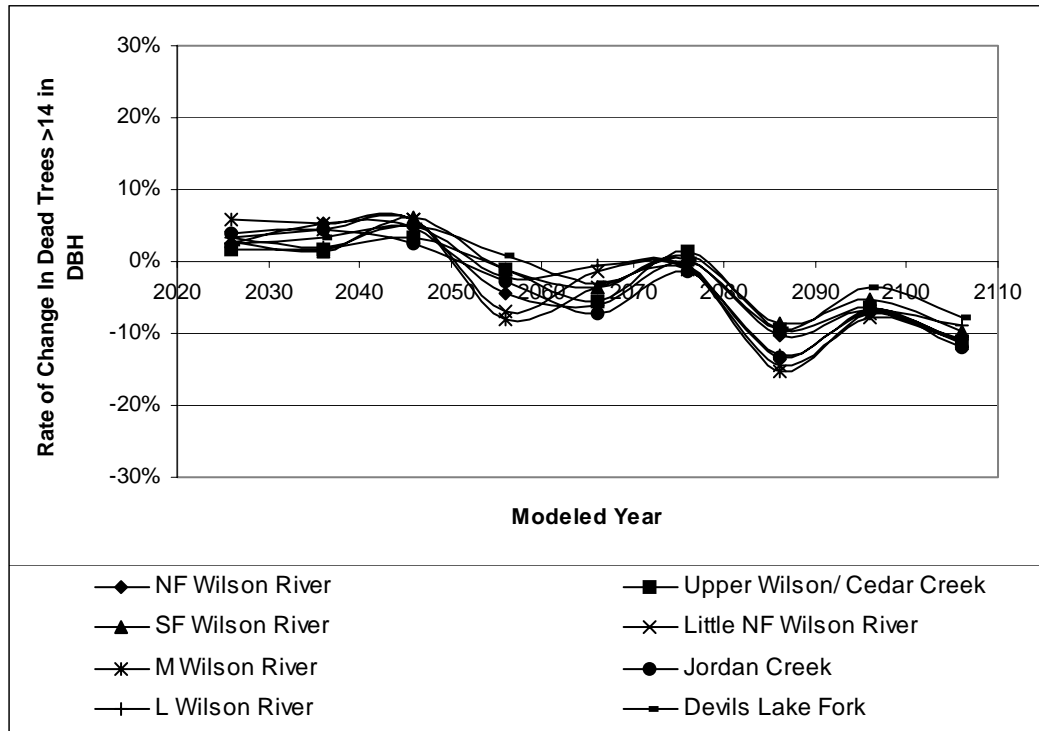


**Figure 107. Model Differences.** Rate of Change in Canopy Tree Mortality. Percent increase or decrease in tree mortality  $\geq 14$  inches DBH, presented as weighted averages by subwatershed.

### 37.1.3.3 Conifer and Hardwood Canopy Mortality

As with live trees, conifer and hardwood mortalities were examined as subsets of the total canopy ( $\geq 14$  inch DBH) mortality values.

**Model #1. Conifer and Hardwood Canopy Mortality (Figure 108 and Figure 111).** Conifer mortality followed that of conifer TPA in a very consistent manner for all subwatersheds. There is a near-term increase in conifer mortality leading in the first 30 years, followed by an even decline for the remainder of the model runs. Total conifer mortality drops to approximately one-half the contributing trees per acre for all subwatersheds through the 100-year time period. Hardwood mortality (Figure 10a) follows a steady increase from years 0-50, followed by an equal decline in the 50-100 year time step. These data illustrate the majority of the dead material being generated by the canopy strata are a hardwood-conifer mix in the first 50 years, followed by dominance in hardwood mortality for the second 50 years.

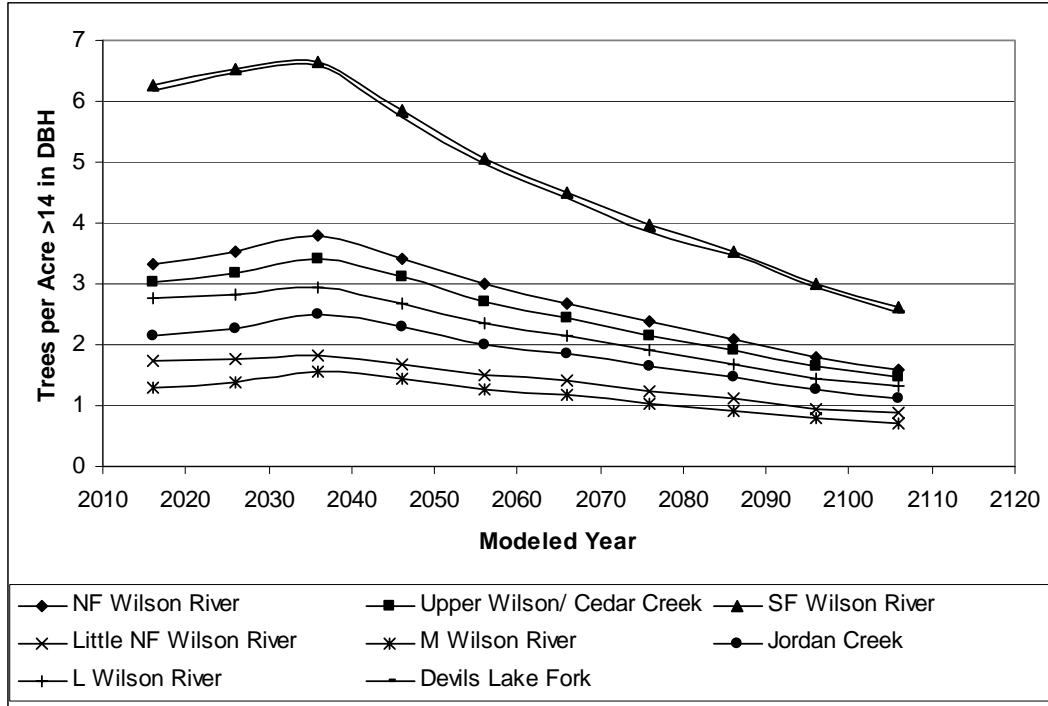


**Figure 108. Model #1.** Projected Canopy Mortality of Conifers. 100-year modeled weighted average of dead trees  $\geq 14$  inches DBH per acre for conifers, by subwatershed.

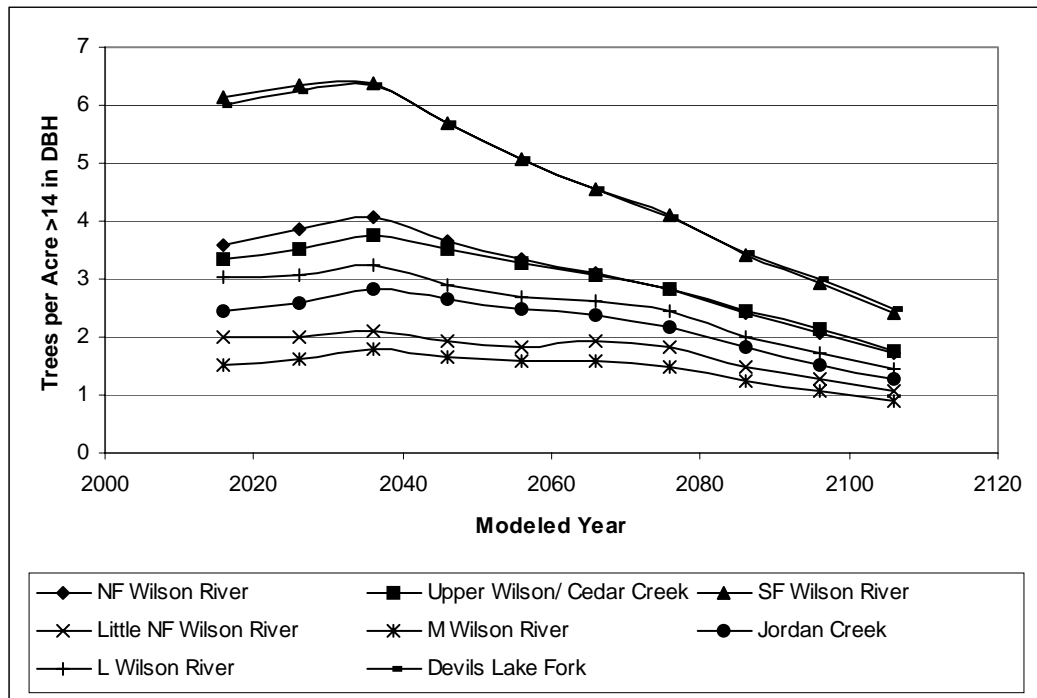


**Figure 109. Model #2.** Projected Canopy Mortality of Conifers. 100-year modeled weighted average of dead trees  $\geq 14$  inches DBH per acre for conifers and hardwoods combined, by subwatershed.

**Model #2. Conifer and Hardwood Canopy Mortality (Figure 109 and Figure 112).** Patterns for Model #2 likewise follow the live TPA trends for conifer densities through time (Figure 109). Steady conifer inputs in the first 30-40 years follow steady declines for the remainder of the model run. The hardwood component (Figure 112) follows a skewed increase peaking at the 50-year time step, followed by a steady decline for the duration of the model run. As with Model #1, the majority of the dead material appears to be hardwood dominant for the 100-year time series, with a higher proportion of dead conifer wood occurring in the first 50 years.

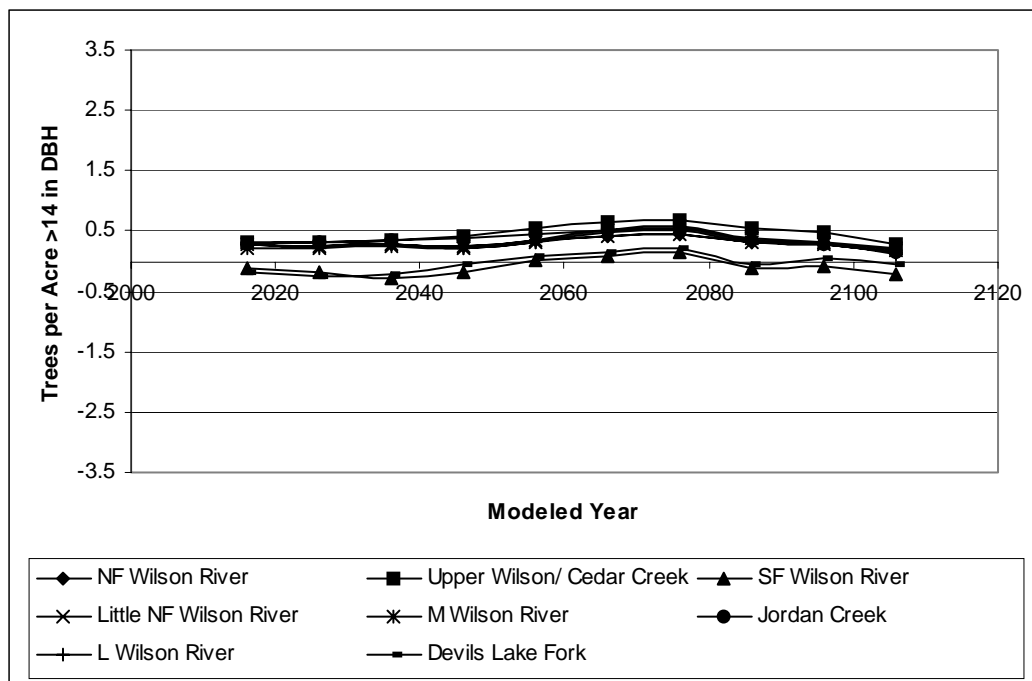


**Figure 110. Model Differences.** Projected Canopy Mortality of Conifers. 100-year modeled weighted average of dead trees  $\geq 14$  inches DBH per acre for conifers, by subwatershed.

**Model Differences. Conifer and Hardwood Canopy Mortality (Figure 110 and Figure 113).** The magnitude in predicted conifer canopy mortality between model runs is very consistent throughout the 100 year time period (Figure 110). There is a slight bias ( $< 0.5$  TPA) for most subwatersheds, though this nominal difference does not change the repeatable conclusion that available dead conifers is declining through time in all subwatersheds. The most notable differences in mortality are in the hardwood component (Figure 113), where Model #2 predicts consistently higher dead wood components through the time series. The steady increases observed in the 0-50 year time step in live trees also corresponds to

higher mortality rates during this time period; this is due to stand density factors in the model. Though there is an increase-decrease pattern in hardwood mortality differences through time, the underlying range is approximately 2 trees per acre of additional hardwoods  $\geq 14$  inches DBH under the Model #2 scenario (adjusted for temporal shift in hardwood peaks). However, by the end of the model run ( $>70$  years), the magnitude differences appear to reverse, with Model #1 producing more hardwood mortality by the end of the 100 year period. The differences in the first 50 years are due to the stand density thresholds of Model #2, and Model #1 begins to show the effects of these thresholds in the  $>70$  year time steps. The understory cohorts are most likely driving this difference.

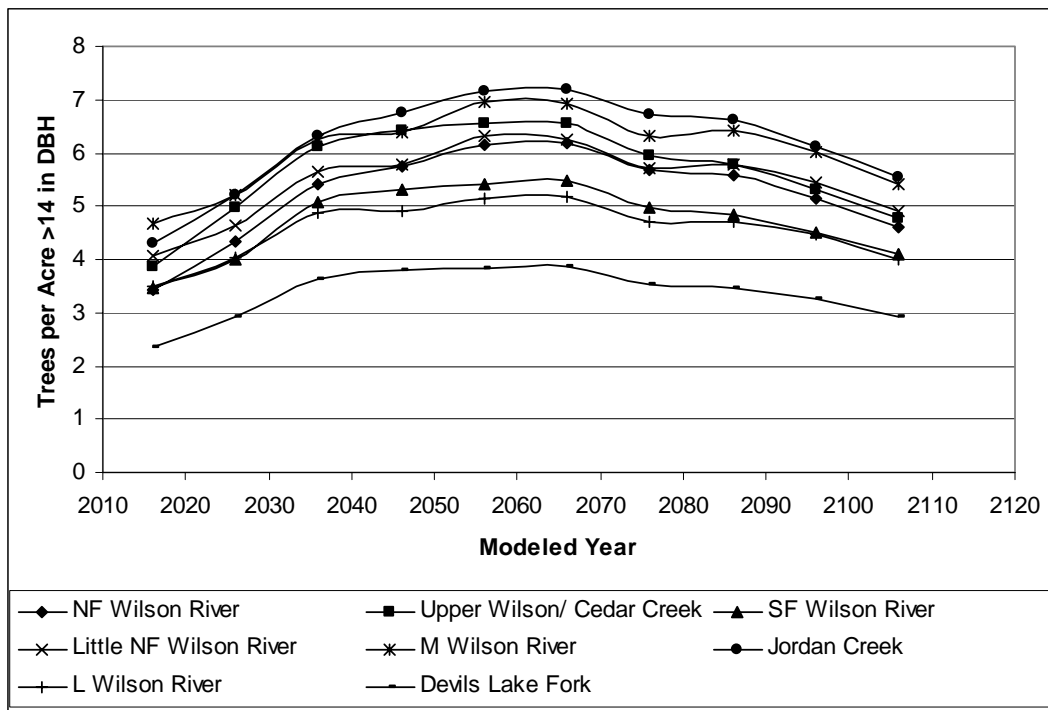


**Figure 111. Model #1.** Projected Canopy Mortality of Hardwoods. 100-year modeled weighted average of dead trees  $\geq 14$  inches DBH per acre for hardwoods, presented by subwatershed.

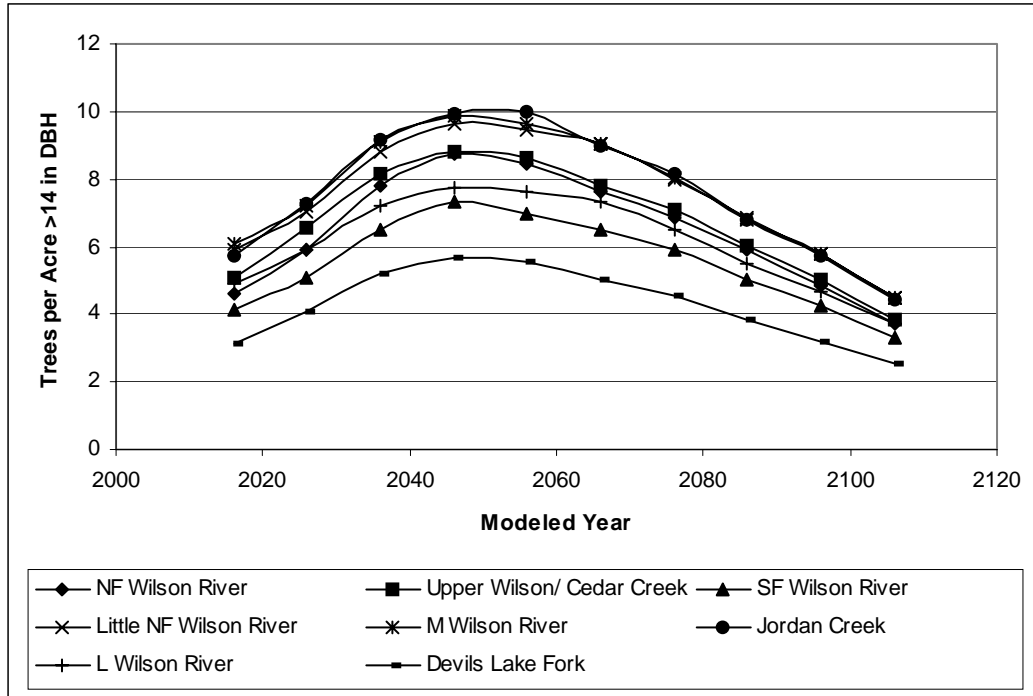


**Figure 112. Model #2.** Projected Canopy Mortality of Hardwoods. 100-year modeled weighted average of dead trees  $\geq 14$  inches DBH per acre for hardwoods, presented by subwatershed.

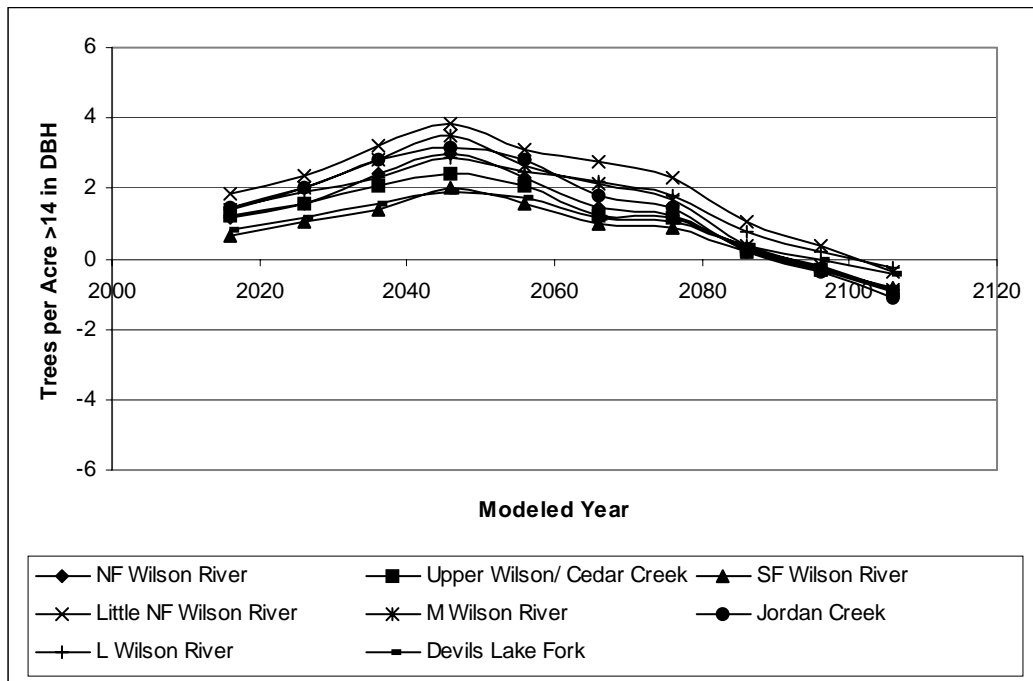


**Figure 113. Model Differences.** Projected Canopy Mortality of Hardwoods. 100-year modeled weighted average of dead trees  $\geq 14$  inches DBH per acre for hardwoods, presented by subwatershed.

### 37.1.4 Compositional Dynamics

Live TPA information for conifers and hardwoods in all size classes was calculated as the ratio of conifer TPA to hardwood TPA and expressed at the subwatershed scale. This value provides an evenly scaled system to evaluate the proportions of conifers within riparian zones, as it normalizes in stand-to-stand differences in TPA magnitude. Specifically, this is one manner by which the relative shifts in species dominance between conifers and hardwoods can be understood through time. Conifer: hardwood ratios were calculated for both model outputs and discussed below.

**Model #1. Conifer: Hardwood Ratio (Figure 113).** Model #1 showed even distributions in conifers and hardwoods throughout the time period. Slight increases in conifer dominance were observed (<0.5%) in the 100 year period, those these values were mostly relegated to the first 50 years, especially during the first few decades, when conifer TPA was increasing. This view effectively displays the shifts in conifer dominance due to mortality events only, as no additional cohorts <5 inches DBH were considered.

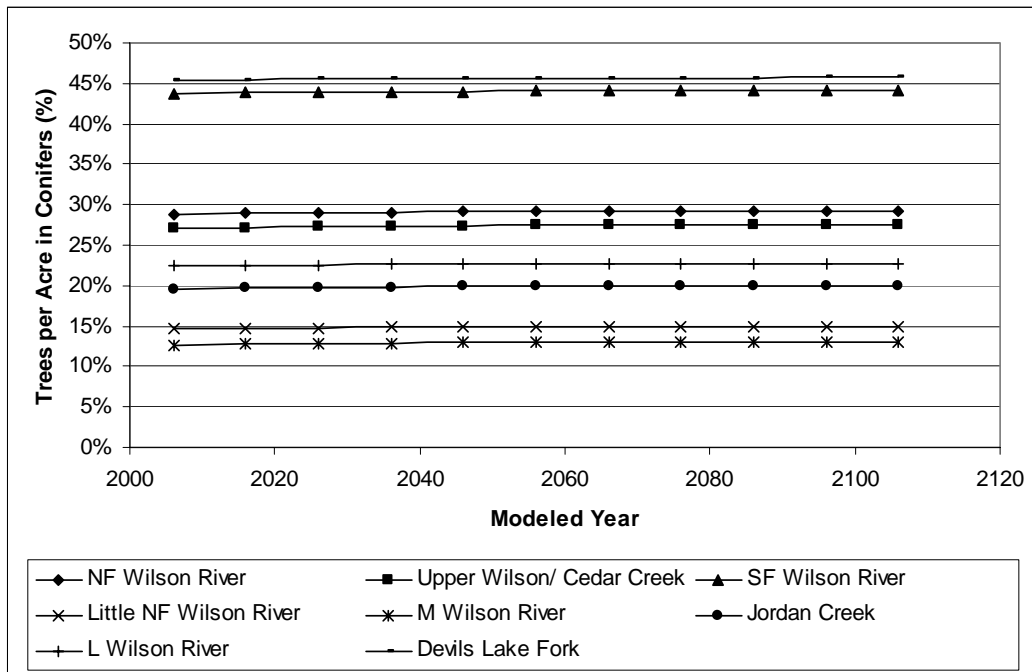


**Figure 114. Model #1.** Relative Abundance of Conifers. Stand-level averages of conifer proportions of trees per acre, weighted at the subwatershed scale.

**Model #2. Conifer: Hardwood Ratio (Figure 115).** The model run shows a clear increase in conifer proportions through time, with a shift in hardwood dominance in the first 50 years to a reversal by the end of the model run. Two major factors contribute to the observed trend. The first is the presence of the 0-5 inch cohort, which contained an element of conifers that are allowed to compete and eventually recruit or persist to later periods of the model run (i.e. when hardwood dominance declines beyond ~50 years). The second, and most significant factor is the regeneration component, and the use of this component during the model run. As stated and explained earlier in this document, the regeneration feature was “forced” natural regeneration, meaning stand density measures did not dictate when seedlings were to be established. This is evidenced by the “stair-step” curves in Figure 115 (and Figure 99), where establishment of seedlings occurred and were subsequently adjusted by mortality triggers relating to stem density, shading, etc. As such, the most persistent species will be projected to survive, favoring conifer species over hardwoods (e.g. hemlock, cedar). Hence, the projection of conifer dominance is mostly dependant upon the assumptions made in regeneration and stand density indices for mortality, and this becomes more important at later periods in the time series.

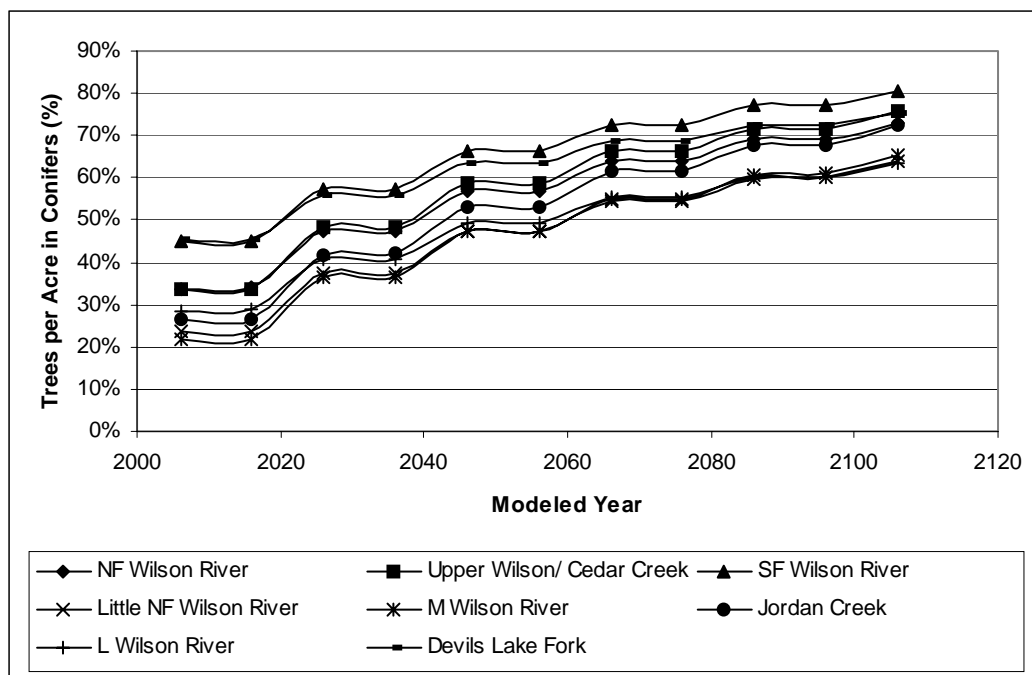


**Figure 115. Model #2. Relative Abundance of Conifers.** Stand-level averages of conifer proportions of trees per acre, weighted at the subwatershed scale.

**Model Differences. Conifer: Hardwood Ratio (No figure presented).** Model differences indicate the proportion of conifers increases through time, attaining dominance in all subwatersheds after year 2057. The model differences are most dependant upon the assumptions of regeneration, and the model parameters defining mortality events. Disturbance events, however, (which are not modeled here) are more significant contributors to compositional dynamics.<sup>4</sup>

### 37.1.5 Key Findings

This analysis provides a view of how two model runs affects riparian forest structure, composition, and mortality through the 100-year time series. In summary of this analysis, the following are key elements that contribute to conclusions in evaluating the differences between model runs:

- Total Stem Density (TPA): Both models are in good agreement with the trending of total TPA through time, with minor temporal changes in stem density peaks. The rate of increase and decrease in TPA are also in good agreement.
- Canopy Composition (TPA): Both models are in good agreement with conifers  $\geq 14$  inches DBH throughout the model run. Slight biases exist, though these biases do not appear to have temporal shifts. Hardwood canopy densities are in good agreement with one another, though there is a  $\sim 10$  year temporal shift in peak abundances on either side of the 50-year time step.
- Understory Composition (TPA): The inherent differences in model assumptions and base data are observed here. Decline in TPA through recruitment out of the  $< 14$  inch size class, or through mortality, is evidenced by Model #1. Model #2 shows a combination of the 0-5 inch size class cohort as well as a ‘forced regeneration’ component and subsequent mortality alternating every 20 years. This model is showing clear “front end loading” of young trees—the trees likely to persist the model criteria associated with shade tolerance and mortality favors conifers (e.g. hemlock).
- Total Canopy Mortality (TPA): Model #2 shows a slight bias for more dead trees for much of the model run. This, in combination with the good agreement in live TPA described above, indicates the stand density-mortality thresholds are controlling the model run. The bias ranges between 1-3 trees per acre on average, mostly in the first 50 years. The

---

<sup>4</sup> Dan Miller, Earth Systems Institute, is the primary specialist for this analysis.

rate of change in canopy mortality is in good agreement, with minor temporal spikes. This suggests the trends in *percent change* in dead canopy trees per acre through time are producing similar outcomes (increase and then decrease in available dead trees peaking at the ~50 year time step).

- **Canopy Mortality Composition (TPA):** There is very good agreement in canopy mortality in conifers. The differences in hardwood trends (i.e. peak years of TPA correspond with peak years in mortality) explain the differences in Total Canopy Mortality (above). The range in hardwood divergence between the models is approximately 2 trees per acre, when temporal shifts in hardwood peak densities are accounted for. The range (not accounting for temporal peaks) is 1-2 for most of the model run and ranges from 2-4 trees per acre at the peak (50 year time step). Model #1 begins to show higher mortality in hardwoods after ~70 years.
- **Compositional Dynamics (conifer: hardwood ratios).** This is a legacy of the models themselves; the primary difference is in the assumptions of how seedlings are regenerated in the model run. As described above, forced natural regeneration favors shade-tolerant conifers, contributing to conifer dominance as time progresses. Further analysis to determine the effect of just the 0-5 inch component (forced natural regeneration excluded) would provide a more reasonable view of composition. Disturbance is the primary function that describes these trends, and it was not modeled as part of this analysis.

### 37.1.6 Conclusions Pertaining to the Watershed Analysis

Overall, the models appear to be in good agreement describing the trends of canopy dynamics. The results show increases in canopy density, followed by decreases to levels at or below the current levels in the 100-year time frame. The magnitude changes affecting LW recruitment and stream shading are potentially modified, though the fundamental question of whether this magnitude brings the current conditions into (or out of) a “desired future condition” is the driving question.

Nominal additional mortality values of 1-3 trees per acre  $\geq 14$  inches DBH at different periods in the time series (Model #2) may change the outcome of the total number of pieces that may interact with the stream channel through time. These pieces appear to be exclusively hardwoods. It is currently not known (though it does not appear likely) if these pieces are sufficient to alter actual LWD inputs to the stream channel or effect overall levels of ecosystem services,

particularly when considering stochastic disturbance patterns will likely have a larger effect on actual inputs than the model differences described here.<sup>5</sup>

The components of stream shading most affected by this analysis are the vegetative structures in tree height, bank overhang, and crown cover. Considering the good agreement in canopy densities through time, it is probable the trends in these values will remain in good agreement. It is possible that the output from Model #2 will influence tree heights, as there are substantially more trees per acre in the understory strata as compared with Model #1. Conversely, the crown cover is likely to be considerably more in Model #2 because of the ‘front-end loading’ of younger cohorts. Whether these two differences will affect “effective shade” (contributing shade by vegetation, topography and stream channel width) at the subwatershed levels remains unknown<sup>6</sup>.

Overall, the model runs support conclusions made that the forested riparian zones will experience a rise-and-fall of hardwood canopy species, and a corresponding ‘lag’ in conifer recruitment to the upper canopy. In addition, the numbers of conifer canopy trees in >20 inch and 35 inch diameter classes are not meeting “standing LWD recruitment” guidelines (per ODFW)<sup>7</sup> in either model case, suggesting the new model run is in support of the management goal recommendations. The duration of the lag period is unknown, though the agreement in canopy dynamics and subsequent rise in conifer ratios by Model #2 support the conclusions that the conifer lag exceeds the 100-year model run under the no-management and no-disturbance scenario.

---

<sup>5</sup> Dan Miller, Earth Systems Institute, is the primary specialist for this analysis.

<sup>6</sup> Ed Salminen, Watershed Professionals Network, is the primary specialist for this analysis.

<sup>7</sup> Model agreement data are available but not presented here.

## 38 Appendix Z – Maps

- Map 1.** Project area, Wilson River watershed, Northwestern Oregon.
- Map 2.** Project area, Wilson River watershed, illustrating the Tillamook and Forest Grove Districts and the eight 6<sup>th</sup> field HUCs.
- Map 3.** Wilson River watershed geologic map grouped by deposit type.
- Map 4.** Industrial forest land ownership in the Wilson River watershed and vicinity.
- Map 5.** Fish bearing streams and the spatial distribution of chum salmon (*Oncorhynchus keta*) within the Wilson River watershed.
- Map 6.** Fish Bearing Streams and the Spatial Distribution of Fall and Spring Chinook (*Oncorhynchus tshawytscha*) within the Wilson River Watershed.
- Map 7.** Fish bearing streams and the spatial distribution of coho salmon (*Oncorhynchus kisutch*) within the Wilson River watershed.
- Map 8.** Fish bearing streams and the spatial distribution of summer and winter steelhead trout (*Oncorhynchus mykiss*) within the Wilson River watershed.
- Map 9.** Land use in the Wilson River watershed and vicinity.
- Map 10.** Spatial distribution of three historic fires that affected the Wilson River watershed.
- Map 11.** Channel disturbance index as defined by NetMap, ESI.
- Map 12.** Probability distribution of headwater sediment yield (PDF Skew) as predicted by NetMap, ESI.
- Map 13.** Coho habitat intrinsic potential (IP) as defined by NetMap, ESI.
- Map 14.** Steelhead habitat intrinsic potential (IP) as defined by NetMap, ESI.
- Map 15.** Coho habitat intrinsic potential (IP) when affected by tributary confluences, wood jams, and wood accumulation. Predicted by NetMap, ESI.
- Map 16.** Core habitat areas for coho salmon as predicted by NetMap, ESI.
- Map 17.** Steelhead core habitat areas predicted by NetMap, ESI.
- Map 18.** Potential biological hotspots defined by NetMap, ESI.
- Map 19.** Channel habitat sensitivity defined by NetMap, ESI..
- Map 20.** Channel modification map of the Wilson River watershed.
- Map 21.** Riparian vegetation Structural Range of Variability.
- Map 22.** Water rights and points of diversion.
- Map 23.** Riparian coverage and general vegetation types in the Wilson River watershed.
- Map 24.** Riparian vegetation types and densities the Wilson River watershed.
- Map 25.** Debris Flow Type F Channels Predicted by NetMAP, ESI.
- Map 26.** Susceptibility to landslide initiation and debris flow delivery to Type F (fish-bearing) streams predicted by NetMAP, ESI.
- Map 27.** Landslide hazard levels based on susceptibility to initiation, delivery to Type F stream, and runout length as Predicted by NetMAP, ESI.
- Map 28.** Channels Most Susceptible to Debris Laden Floods predicted by NetMAP,
- Map 29.** Debris Flow Type N Channels Predicted by NetMAP, ESI.
- Map 30.** The Minimum Wood Diameter required to form pools along a specific channel.
- Map 31.** Functional Wood Abundance for Year 2036 (# pieces / 100m). Unsampled riparian stand types not shown.

- Map 32.** Functional Wood Abundance for Year 2056 ( # pieces / 100 m). Unsampled riparian stand types not shown.
- Map 33.** Functional Wood Abundance for Year 2106 ( # pieces / 100 m). Unsampled riparian stand types not shown.
- Map 34.** Debris Flow Susceptibility Reaches
- Map 35.** Reaches Sensitive to Debris Flow Inputs with High to Moderate Debris Flow Susceptibility and Low Riparian Wood Recruitment; Simulation Year 2056
- Map 36.** Does Not Exist.
- Map 37.** High Priority Fish Bearing Reaches.
- Map 38.** High Priority Reaches and Areas of Expected Landslide Delivery to Streams, NetMAP, ESI.
- Map 39.** High Priority Reaches Illustrating Expected Debris-Flow Track Length
- Map 40.** Wetland types of the Wilson River watershed.
- Map 41.** Populations of Japanese knotweed in the Wilson River watershed.
- Map 42.** Dispersed campsites ranked by overall impact.
- Map 43.** Dispersed campsites within 25 feet of streams.
- Map 44.** Shallow Landslide Susceptibility Predicted by NetMAP, ESI.
- Map 45.** Predicted deep seated landslide potential for the Wilson River watershed, NetMap, ESI.
- Map 46.** Road status on ODF lands in the Wilson River watershed.
- Map 47.** Roads classified as hydrologically connected in the eastern portion of the Wilson River watershed.
- Map 48.** Roads classified as hydrologically connected in the western portion of the Wilson River watershed.
- Map 49.** Critically located roads categorized by stream severity.
- Map 50.** Critically located roads categorized by slope severity.
- Map 51.** Road prism stability on ODF lands in the eastern portion of Wilson River watershed.
- Map 52.** Road prism stability on ODF lands in the western portion of Wilson River watershed.
- Map 53.** Stream crossing washout potential on ODF lands in the Wilson River watershed.
- Map 54.** Road washouts surveyed by the Tillamook District road engineers after the storm of November 2006.
- Map 55.** Hydrologically connected recreation trails surveyed in 2006.
- Map 56.** Prism stability categories for surveyed trails.
- Map 57.** Fish barriers at stream crossings on the eastern portion of the Wilson River watershed.
- Map 58.** Fish barriers at stream crossings on the western portion of the Wilson River watershed.
- Map 59.** Channel Classification System #1 as determined using NetMap, ESI.
- Map 60.** Channel Classification System #2 as determined using NetMap, ESI
- Map 61.** Current Vegetation Classification
- Map 62.** Potential Vegetation Classification
- Map 63.** High-density conifer stands with large diameter trees on sites with high landslide risk.